2

Synthesis of cage alkenes as possible monomers for ROMP

2.1. Potential cage monomers for ROMP

Cage monomers that are potentially suitable as substrates for ROMP may be divided into two groups according to the position of the double bond in the structure (**Figure 2.1**). Endocyclic cage alkenes are those with double bonds located within the cage framework. In a broad sense this category includes compounds with rigid cycloalkenyl fragments.

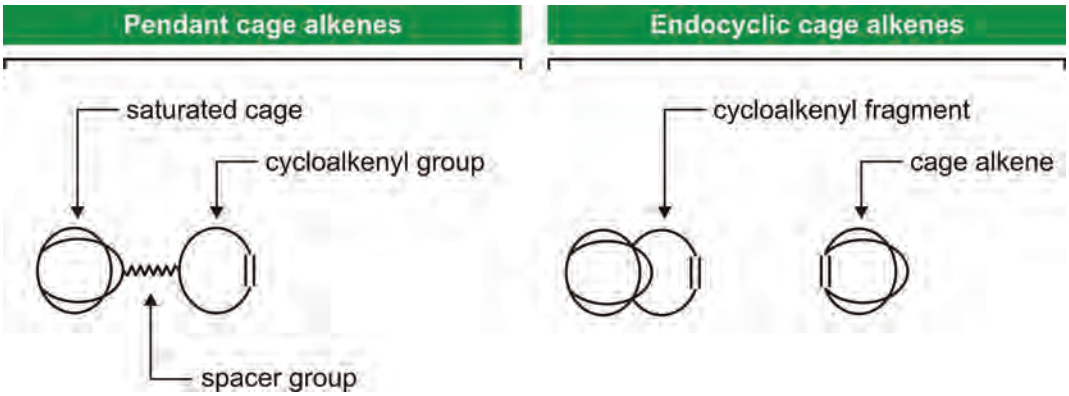

Figure 2.1: Classifications of cage alkenes suitable for ROMP.

The aim of this part of the study was to synthesise new and previously reported endocyclic cage alkenes that could potentially serve as monomers in ROMP reactions. The reactivities of these compounds were subsequently tested with commercially available well-defined ruthenium carbene catalysts. The results of these tests are reported in the next chapter (➡ p. 75).

2.1.1. Examples of endocyclic cage alkenes

The endocyclic cage alkenes reported in the literature mostly functioned as intermediates in larger synthetic schemes. A notable exception is the attempted synthesis of adamantene (**92**).[136-139] Calculations have shown that the sp^2-carbon atoms of **92** are not in the same plane and that sufficient overlap of the p-orbitals will be accompanied by significant deformation of the rigid cage framework.[136] Consequently, adamantene is expected to have a transitory existence only. Some attempts to provide evidence for the existence of **92** are shown in **Scheme 2.1**. Treatment of 1,2-

diiodoadamantane (**90**) with n-butyllithium yielded the dimer **93** in 98% yield.[140] Alberts *et al*.[136] were able to trap adamantene as the adduct **95** by heating the bis-*t*-butylperester **91** in a solution of 2,5-dimethylfuran (**94**).

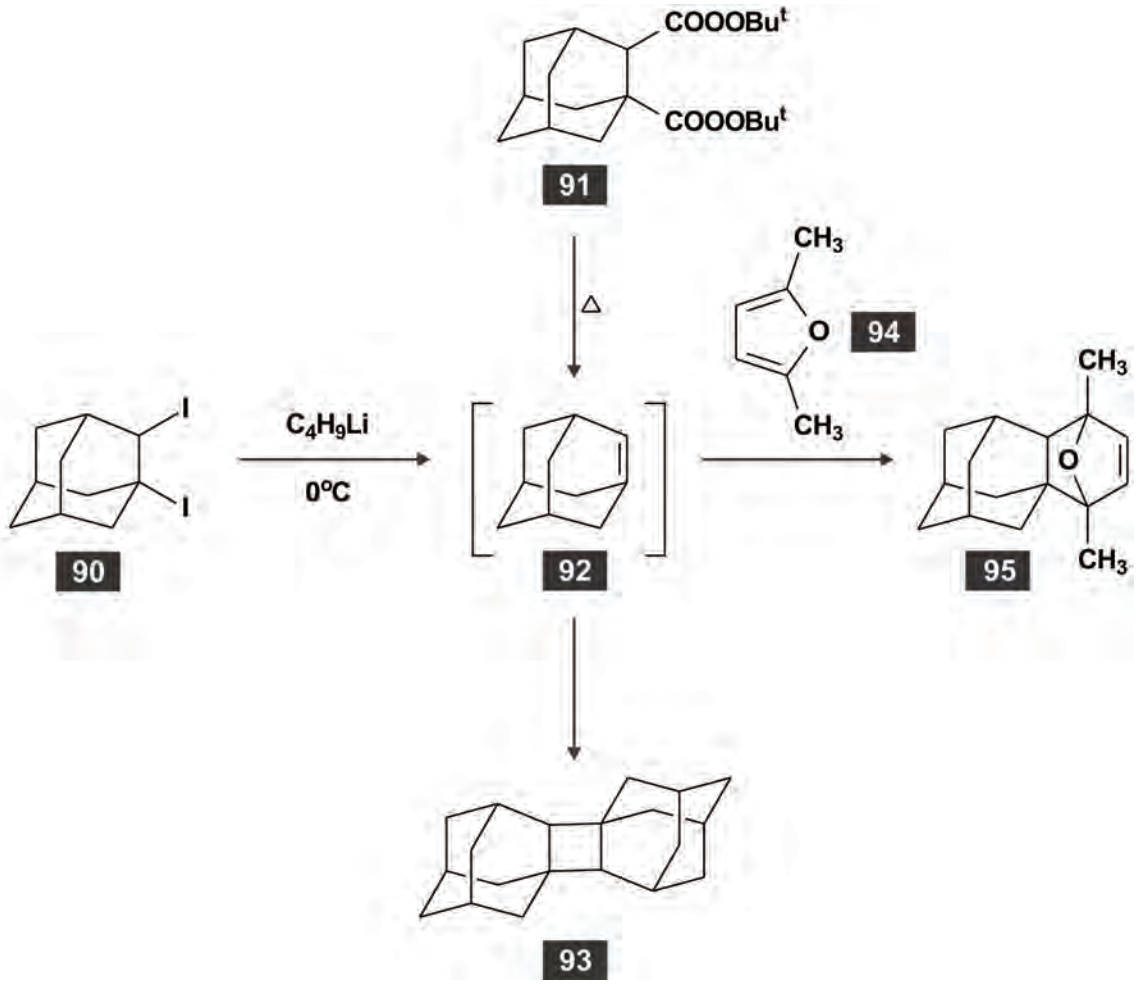

Scheme 2.1: Attempted synthesis of adamantene.

The tendency of double bonds to avoid bridgehead positions has been summarised as Bredt's rule.[141] Although there are exceptions[142] to this rule, it may still serve as a useful guideline when embarking on the synthesis of new endocyclic cage alkenes. Maier and Schleyer[143] found that the fraction of the total strain contributed by the twist of the carbon-carbon double bond is a reliable indicator of the stability of a bridgehead alkene. So-called *anti*-Bredt cage alkenes will probably not be practical candidates for ROMP investigations.

Diels-Alder reactions provide a direct means to incorporate one or more double bonds into cage structures. An example of this approach is provided by the synthesis of hexacyclo[7.4.2.0^{1,9}.0^{3,7}.0^{4,14}.0^{6,15}]pentadecane-10,12-diene-2,8-dione (**98**, **Scheme 2.2**).[144-145] In this example the cage alkene may function as a diene and an additional Diels-Alder reaction may

be used to incorporate a new double bond into the cage framework. The stereochemical behaviour (π-facial selectivities) of Diels-Alder reactions involving **98** have been thoroughly investigated.[146] It was found that the reactions of **98** with olefinic dienophiles occur mostly by attack on the carbonyl-bearing face of the diene fragment to yield the adduct **99a** (**Scheme 2.2**).

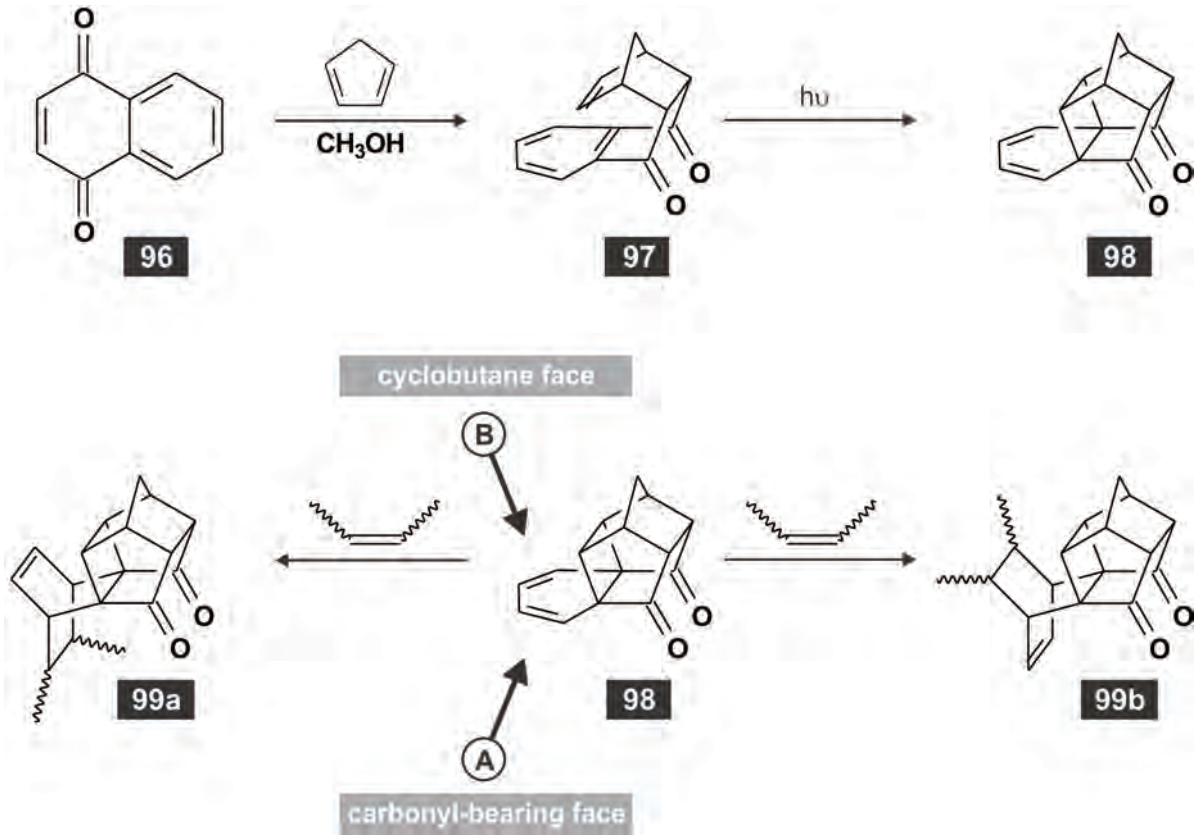

Scheme 2.2: The use of Diels-Alder reactions in the synthesis of endocyclic cage alkenes.

The Diels-Alder reactions can also be used to construct adducts with suitably orientated double bonds that would yield an endocyclic cage alkene upon irradiation. This approach is exemplified by the procedures shown in **Scheme 2.3** and **Scheme 2.4**.

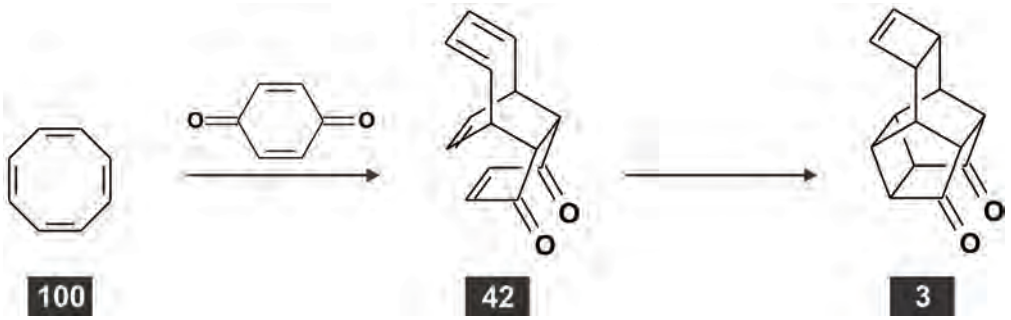

100 42 3

Scheme 2.3[147]**:** Synthesis of hexacyclo[8.4.0.$0^{2,9}$.$0^{3,13}$.$0^{4,7}$.$0^{4,12}$]tetradec-5-en-11,14-dione.

The cycloaddition of 1,3,5,7-cyclooctatetraene (COT) to 1,4-benzoquinone produced the adduct **42** upon stirring in *o*-dichlorobenzene at high temperature.[147] Irradiation of **21** in hexane produced the cage alkene **3** in high yield (**Scheme 2.3**). The Diels-Alder reaction of the dione **101** with cyclopentadiene produced a mixture of the *endo*-adduct **102** and *exo*-adduct **103**.[148] These were transformed to the *anti*-compound **104** and *syn*-compound **105**, respectively (**Scheme 2.4**). Compounds **3**, **104** and **105** may possess high degrees of ring strain that could make them suitable candidates for ROMP.

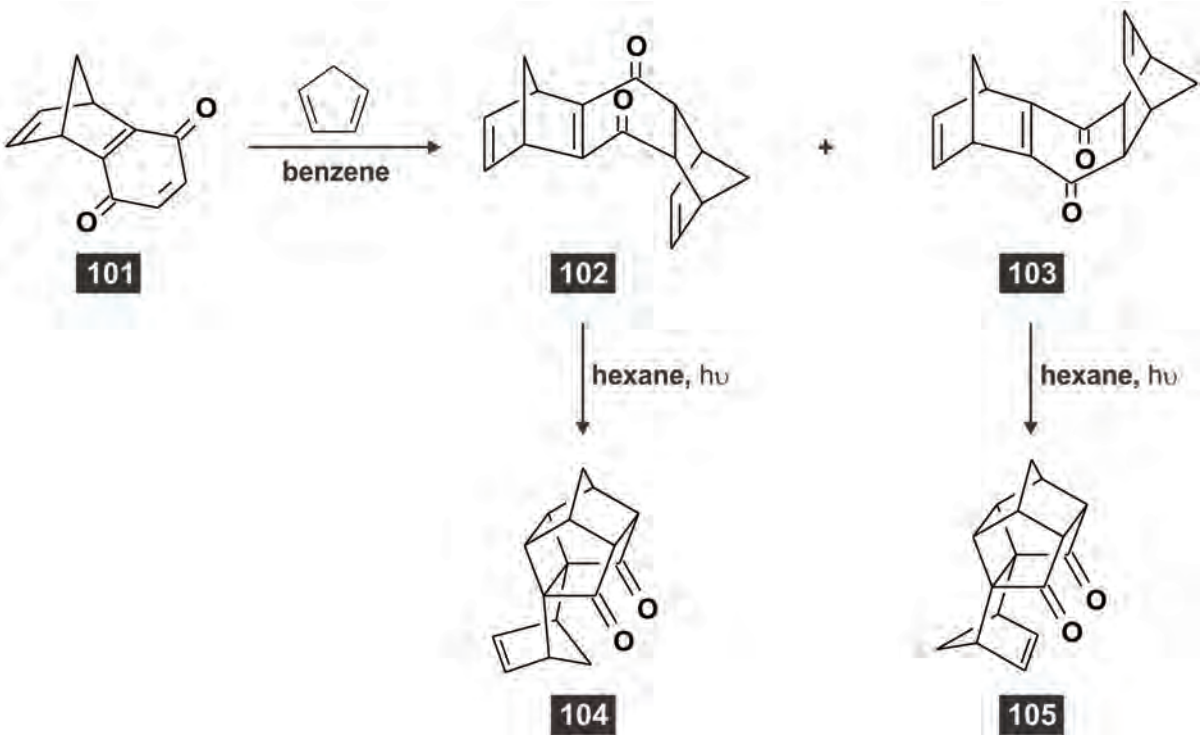

Scheme 2.4[148]**:** Synthesis of heptacyclo[1.0.2.1.$1^{5,8}$.$0^{2,11}$.$0^{4,9}$.$0^{2,6}$.$0^{7,11}$]hexadec-13-en-3,10-dione.

Part of the synthesis of hexacyclo[6.5.1.$0^{2,7}$.$0^{3,11}$.$0^{4,9}$.$0^{10,14}$]tetradeca-5,12-diene[149] (**114**) is shown in **Scheme 2.5**. It is apparent that 2,4-cyclopentadien-1-one (**106**) could have been an ideal diene for construction of this cage compound. Unfortunately, **106** is an elusive compound that immediately forms the dimer **107** upon generation.[150] The instability of **106** has been ascribed to antiaromatic character.[151] However, it has been observed that substituted cyclopentadienones with three or more substituents do not dimerise or form dimers that are capable of dissociation.[152] Thus, a synthesis approach employed to circumvent the problem posed by the instability of **106** comprises the use of a substituted cyclopentadienone from which undesired substituents can be removed later. The diene 1,2,3,4-tetrachloro-5,5-dimethoxy-1,3-cyclopentadiene[153] (**10**) is often used as a synthon for cyclopentadienone (**Scheme 2.5**). This diene ultimately produces a cage compound with a ketal functionality that can be hydrolysed to a carbonyl group. The chlorine atoms can be removed from the cage compound by reductive dehalogenation.[154-155]

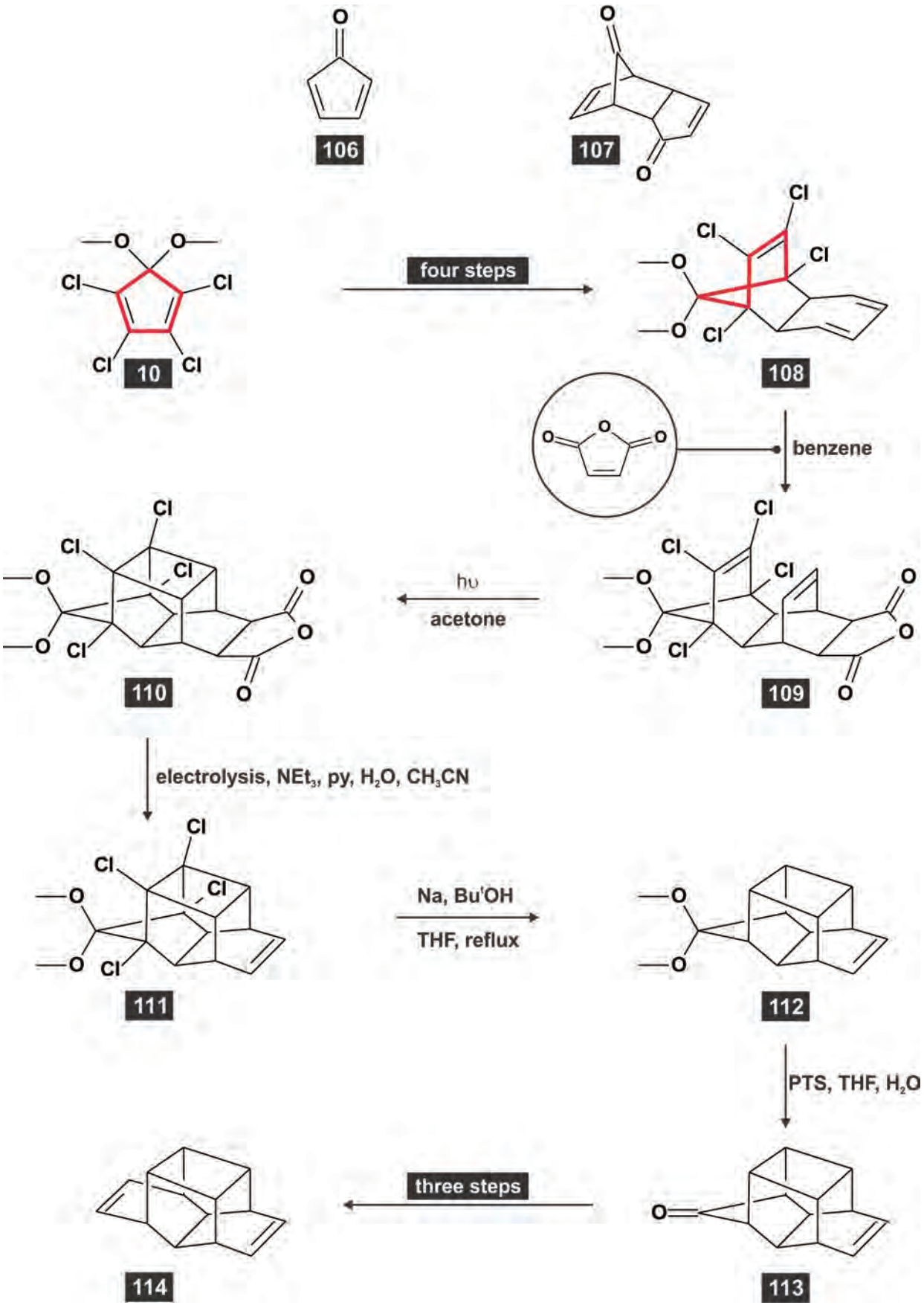

Scheme 2.5[149]**:** Synthesis of hexacyclo[6.5.1.$0^{2,7}$.$0^{3,11}$.$0^{4,9}$.$0^{10,14}$]tetradeca-5,12-diene.

Eaton *et al*.[51] reported (**Scheme 2.6**) two endocyclic cage alkenes, tetracyclo[6.3.0.0^{4,11}0^{5,9}]undec-2-en-6-one (**1**) and tetracyclo[6.3.0.0^{4,11}0^{5,9}]undec-2,6-diene (**120**), in their successful attempt to synthesise homopentaprismane (**39**). The bromoketone **117** underwent reductive dehalogenation in the presence of zinc and acetic acid to produce the ketoalkene **1**, while dehydrohalogenation of **119** yielded the diene **120**.

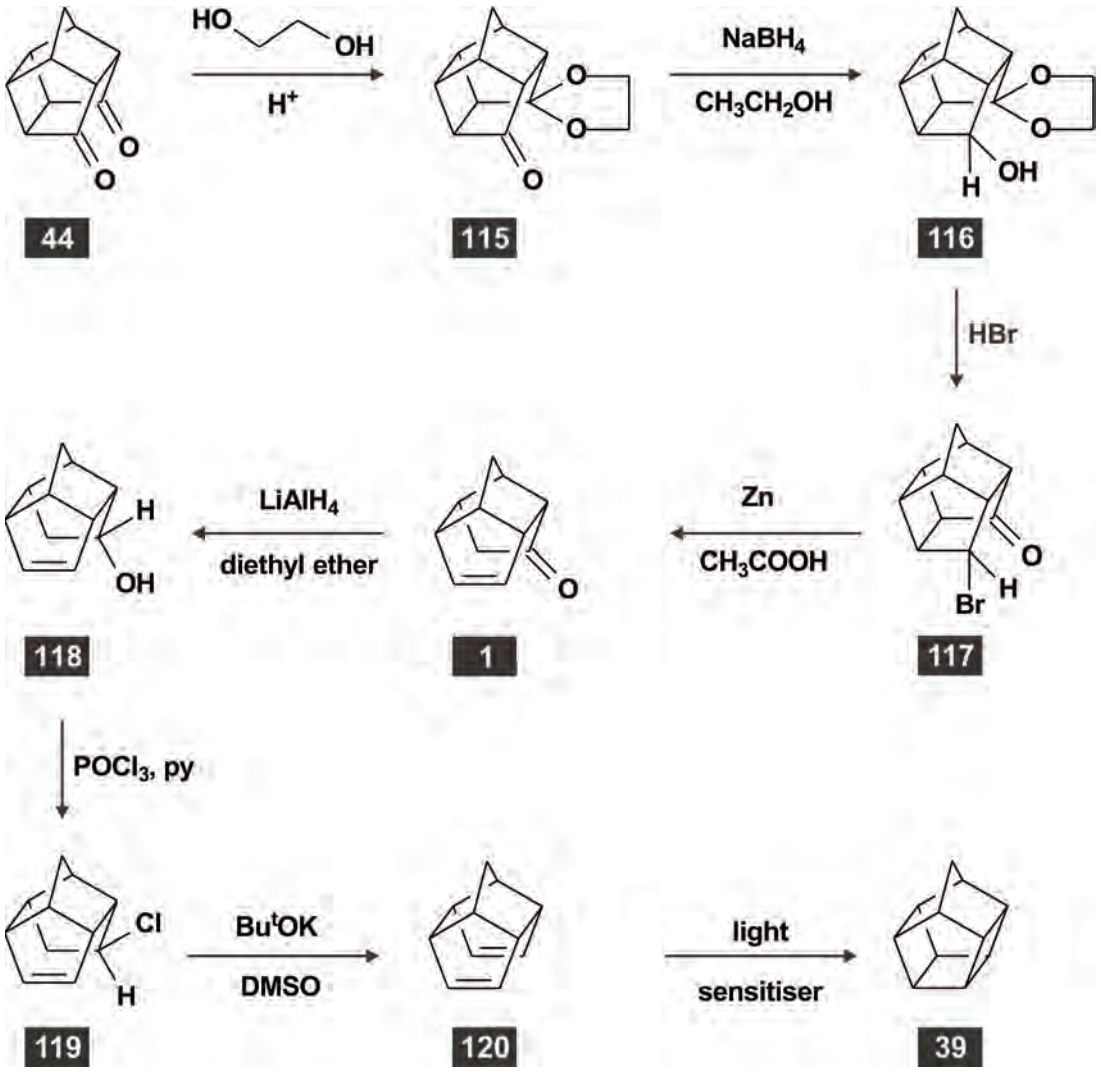

Scheme 2.6[51]**:** Synthesis of tetracyclo[6.3.0.0^{4,11}0^{5,9}]undec-2-en-6-one.

2.2. Synthesis of derivatives of tetracyclo[6.3.0.0^{4,11}0^{5,9}]undec-2-en-6-one

The carbonyl group of tetracyclo[6.3.0.0^{4,11}0^{5,9}]undec-2-en-6-one (**1**) presented an ideal opportunity to synthesise cage alkenes with different functional groups. The derivatives considered in this study is summarised in **Table 2.1**. These compounds could ultimately be used to explore the possible influence of functional groups on the ROMP reactivity of cage alkenes.

Table 2.1: Derivatives prepared from ketoalkene 1

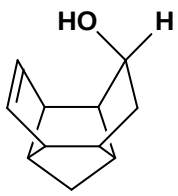	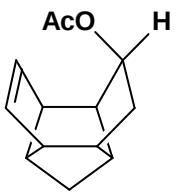	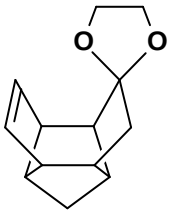
118[51]	**121**	**122**
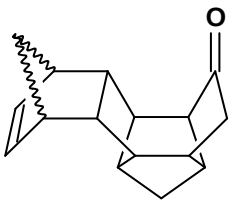	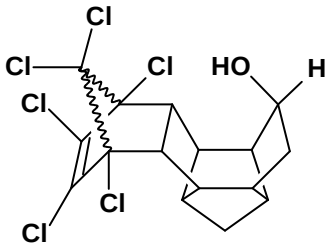	
123	**124**	
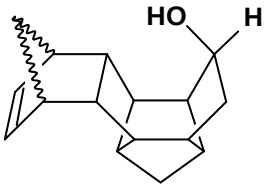	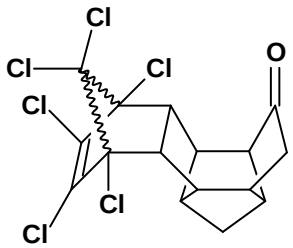	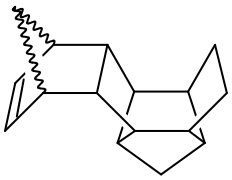
125	**126**	**127**

The ketoalkene **1** and hydroxyalkene **118** were prepared according to methods reported in the literature.[51] In addition, the previously unreported derivatives **121** and **122** were synthesised (**Scheme 2.7**).

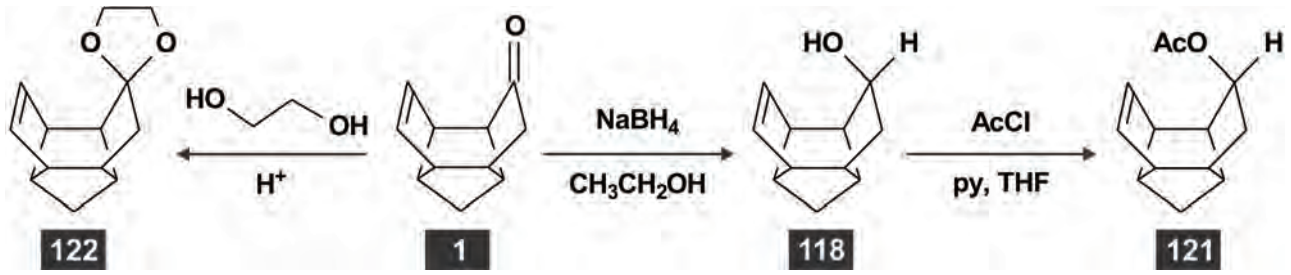

Scheme 2.7: Synthesis of derivatives of tetracyclo [6.3.0.0^{4,11}0^{5,9}]undec-2-en-6-one.

Nuclear magnetic resonance (NMR) spectroscopy has evolved into a powerful tool for elucidating the structures of organic compounds. The 150 MHz ^{13}C NMR spectrum of the ketoalkene **1** shows eleven signals that can be associated with eleven non-equivalent carbon atoms. The signal at δ_c 221.2 is due to the carbonyl group and those at δ_c 136.4 and δ_c 137.8 can be ascribed to the

presence of two olefinic carbon atoms. The 600 MHz ^{1}H NMR spectrum of **1** shows two AX spin systems that represent two different methylene groups. Comparison of the coupling constants allowed discrimination between these methylene groups. It has been shown that the coupling constants of bridgehead methylene protons of pentacycloundecane (PCU) derivatives are approximately 10 Hz.[156-160] Based on these observations, the doublet signals at 1.75 ppm and 1.80 ppm ($^{2}J_{a,s}$ = 11.1 Hz) were assigned to the methylene protons of C-10. The bridgehead methylene proton H-10$_a$ (δ_H 1.75) resonates at lower frequency than H-10$_s$ (δ_H 1.81).[156-159] A coupling constant of approximately 18 Hz can be expected for a methylene group situated next to a carbonyl group.[161] Furthermore, based on the Karplus relationship,[162-163] the ^{3}J coupling constant for coupling between H-8 and H-7$_a$ should be approximately 6 Hz. Therefore, the signal at δ_H 2.00 (doublet, $^{2}J_{a,s}$ = 18.4) and δ_H 2.15 (doublet of doublets, $^{2}J_{a,s}$ = 18.4, $^{3}J_{H\text{-}8,H\text{-}7a}$ = 5.9) can be assigned to the protons H-7$_s$ and H-7$_a$, respectively. The correlation spectroscopy (COSY) spectrum of **1** shows correlations between the protons at H-10 (δ_H 1.75 and δ_H 1.81) and the signals at 2.84 ppm (H-9) and 3.05 ppm (H-11). The signals of H-7 (δ_H 2.00 and δ_H 2.15) correlate with the doublet at 2.35 ppm (H-8). The latter shows correlations with δ_H 2.84 (H-9) and δ_H 2.77 (H-1). The signal at 3.05 ppm (H-11) also correlates with the signal at δ_H 2.77 and can therefore be assigned to H-1. The signals at δ_H 6.04 and δ_H 5.95 are due to the olefinic protons H-2 and H-3. The signal at δ_H 6.04 can then be assigned to H-2 because of the correlation with H-1 (δ_H 2.77). The assignments of the remaining signals in the ^{1}H NMR and ^{13}C NMR spectra followed from COSY and Heteronuclear Multiple Quantum Coherence (HSQC) data and are shown in **Table 2.2**.

Table 2.2: ^{1}H and ^{13}C NMR data^{x} of 1

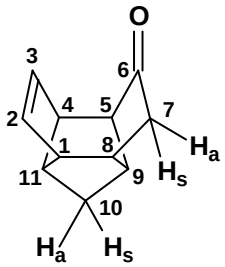

1

Number C/H	δ^{y}_{H} (ppm)	J (Hz)	δ^{y}_{C} (ppm)
1	2.77	-	50.1
2	6.04	-	137.8
3	5.95	-	136.4
4	2.61	-	46.4
5	2.45	-	38.5
6	-	-	221.2
7$_a$	2.15	18.4 ($^{2}J_{a,s}$) 5.9 ($^{3}J_{H\text{-}8,H\text{-}7a}$)	42.6
7$_s$	2.00	18.4 ($^{2}J_{as}$)	
8	2.36	-	56.1
9	2.84	-	52.0
10$_a^{z}$	1.75	11.1 (^{2}J)	33.9
10$_s^{z}$	1.81	11.1 (^{2}J)	
11	3.05	-	59.8

x ^{1}H NMR spectrum: 600 MHz, ^{13}C NMR spectrum: 150 MHz

y Solvent: $CDCl_3$

Attempts were made to convert the ketoalkene **1** to the ketal **122**. Refluxing **1** with ethylene glycol and a catalytic amount of PTS in toluene produced a complex mixture of compounds. The same inclination towards by-product formation was also observed when acetylation of the cage alcohol **118** was attempted with acetic anhydride and a catalytic amount of PTS.[164] Analysis with GC-MS indicated the formation of at least four isomeric products. These results suggested that PCU cage alkenes may be prone to by-product formation under acid conditions. The ketal **122** was not isolated and no further acid medium reactions were attempted with **1** or its derivatives.

Reduction of the ketoalkene **1** yielded the hydroxyalkene **118** (**Scheme 2.7**).[51] The assignments of the signals in the ^{1}H NMR and ^{13}C NMR spectra of **118** followed in a way similar to that already described for **1** and are shown in **Table 2.3**.

Table 2.3: ^{1}H and ^{13}C NMR data[x] of 118

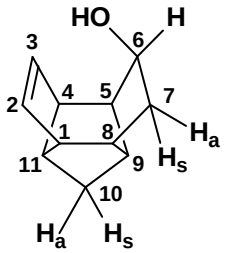

118

Number C/H	δ^{y}_{H} (ppm)	J (Hz)	δ^{y}_{C} (ppm)
1	2.55	-	47.7
2	6.03	-	139.9
3	6.39	-	139.4
4	2.47	-	51.6
5	2.27	-	52.4
6	4.45	-	77.5
7_a	1.48	14.2 (^{2}J) 4.6 (^{3}J)	39.0
7_s	2.27	- [z]	
8	2.13	-	42.4
9	2.47	-	46.7
10_a	1.54	10.9 (^{2}J)	32.3
10_s	1.57	10.9 (^{2}J)	59.4
11	2.91	-	
OH	1.80	-	-

[x] ^{1}H NMR spectrum: 600 MHz, ^{13}C NMR spectrum: 150 MHz

[y] Solvent: $CDCl_3$

[z] Coupling constant could not be determined due to overlap of these proton signals.

The geminal hydrogen atoms at C-7 register at δ_H 1.48 and δ_H 2.27. The COSY spectrum of **118** shows a correlation between the signals at δ_H 2.13 (H-8) and δ_H 2.27. This correlation is possible only if the proton registering at δ_H 2.27 has an *anti*-orientation. Therefore, the signal at δ_H 2.27 is assigned to H-7_a. The COSY spectrum of **118** also shows a correlation between the signals at δ_H 2.27 (H-5) and δ_H 4.45 (H-6). Once again this correlation is possible only if the orientation of H-6 is *anti*. The observed correlations imply that the signal at δ_H 4.45 represents a hydrogen atom with *anti*-orientation and that the hydroxyl group is orientated *endo*. The predicted value of the vicinal coupling constant for coupling between H-7_s and H-6 is approximately 5 Hz. Reasonable

agreement between the estimated value and experimental value of ^{3}J supports the assigned orientation of H-6 and by implication the *endo*-orientation of the hydroxyl group.

Although several reagents are available for the acetylation of alcohols, a mixture of acetic anhydride and pyridine is commonly used for this purpose.[165-166] Bases more efficient than pyridine may be used in the acetylation procedure, but these are more expensive.[167] Treatment of **118** with a mixture of acetic anhydride and pyridine led to incomplete conversion to the acetate **121**. A conversion of 73% was only achieved after a fresh aliquot of the reagent was added for the third time. Although the reaction produced a fair percentage of **121**, the reaction was slow and required an excess amount of acetic anhydride. The use of acetic anhydride in the presence of a catalytic amount of iodine[168] did not improve the situation and only led to 50% conversion to product after three days. Subsequently, acetylation with acetyl chloride in dry pyridine was considered.[169-170] Treatment of **118** with acetyl chloride in dry pyridine produced a 78% yield of **121** in a single run. Acetyl chloride in pyridine is the superior reagent for acetylation of the hydroxyalkene **118**.

The IR spectrum of **121** exhibits a carbonyl group absorption at 1727 cm^{-1} and the characteristic C-C(=O)-O band at 1237 cm^{-1}. The mass spectrum shows a molecular ion at *m/z* 204 that supports a molecular formula of $C_{13}H_{16}O_2$. Assignments of the different resonance signals in the ^{1}H NMR and ^{13}C NMR spectra of **121** to specific nuclei are given in **Table 2.4**.

Table 2.4: ^{1}H and ^{13}C NMR data[x] of 121

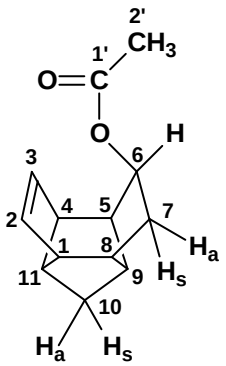

121

Number C/H	δ^{y}_{H} (ppm)	J (Hz)	δ^{y}_{C} (ppm)
1	2.47	-	47.5
2	5.81	-	136.0
3	6.15	-	140.6
4	2.40	-	46.6
5	2.33	-	49.5
6	5.12	-	78.5
7_a	2.20	-[z]	35.4
7_s	1.63	14.4 (^{2}J) 4.7 (^{3}J)	
8	2.09	-	41.9
9	2.47	-	51.1
10_a	1.52	10.9 (^{2}J)	32.1
10_s	1.55	10.9 (^{2}J)	
11	2.84	-	58.5
1'	-	-	171.1
2'	2.01	-	21.3

[x] ^{1}H NMR spectrum: 600 MHz, ^{13}C NMR spectrum: 150 MHz

[y] Solvent: $CDCl_3$

[z] Coupling constant could not be determined due to overlap of these proton signals.

The 150 MHz ^{13}C NMR spectrum ($CDCl_3$) of **121** shows signals that may be associated with thirteen different carbon atoms. The signal of the carbonyl carbon atom registers at δ_C 171.1 and the methyl carbon atom registers at δ_C 21.3. The 600 MHz ^{1}H NMR spectrum ($CDCl_3$) of **121** shows the methylene protons of C-10 as an AB spin system at δ_H 1.52 (J = 10.9 Hz) and δ_H 1.55 (J = 10.9 Hz) that again served as the starting point for assignment of the signals registered for the PCU framework. The methyl protons of the acetyl group registers at δ_H 2.01 due to the proximity of the carbonyl group. The orientation of the acetate group was established in a way similar to that described for the hydroxyl group of **118**.

2.2.1. Synthesis of cage alkenes utilising the Diels-Alder reaction

Scheme 2.8 summarises the utilisation of the Diels-Alder reaction to prepare cage alkenes from tetracyclo[6.3.0.0^{4,11}0^{5,9}]undec-2-en-6-one (**1**).

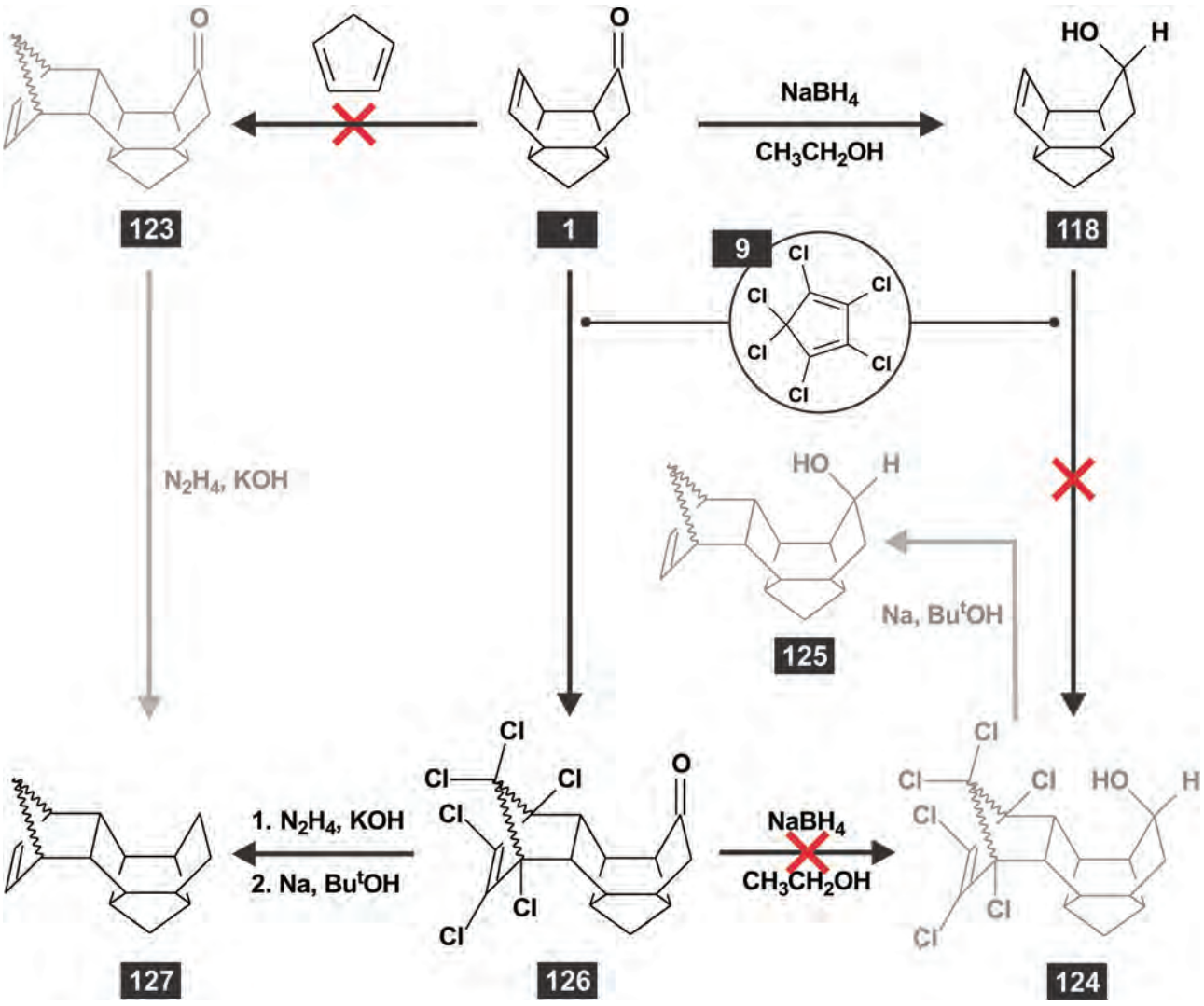

Scheme 2.8: Utilisation of the Diels-Alder reaction to synthesise cage alkenes.

The simplest route to **127** appeared to be the reaction of the ketoalkene **1** with cyclopentadiene followed by removal of the carbonyl group (**Scheme 2.8**). However, it seemed more probable that cyclopentadiene would dimerise than react with the bulky dienophile **1**. GC-MS analysis of the reaction mixture confirmed the presence of dicyclopentadiene and unreacted ketoalkene **1**.

The reaction of **1** with hexachlorocyclopentadiene (**9**) in refluxing toluene afforded the adduct **126** in fair yield (43%). The mass spectrum of **126** shows a molecular ion at *m/z* 432 that supports a molecular formula of $C_{16}H_{12}Cl_6O$. The IR spectrum shows a weak carbonyl group absorption at 1724 cm^{-1}. Assignments of the resonance signals in the ^{1}H NMR spectra and ^{13}C NMR spectra of **126** to specific nuclei are given in **Table 2.5**.

Table 2.5: ^{1}H and ^{13}C NMR data[x] of 126

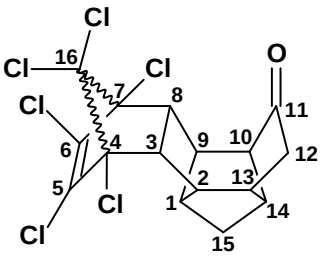

126

Number C/H	δ^{y}_{H} (ppm)	J (Hz)	δ^{y}_{C} (ppm)
1	2.45	-	47.9
2	2.34	-	40.7
3	3.06	-	55.6
4	-	-	80.8 or 80.9
5	-	-	130.99 or 131.01
6	-	-	130.99 or 131.01
7	-	-	80.8 or 80.9
8	3.06	-	56.1
9	2.48	-	46.2
10	2.50	-	56.5
11	-	-	220.1
12_a	2.21	19.3 (^{2}J)	41.0
12_s	2.35	19.3 (^{2}J) 6.5 (^{3}J)	
13	2.66	-	41.0
14	2.62	-	46.3
15_a	1.68	11.3 (^{2}J)	33.6
15_s	1.76	11.3 (^{2}J)	
16	-	-	104.2

x ^{1}H NMR spectrum: 600 MHz, ^{13}C NMR spectrum: 150 MHz

y Solvent: $CDCl_3$

The 150 MHz ^{13}C NMR spectrum ($CDCl_3$) of **126** shows signals that may be associated with sixteen different carbon atoms with the carbonyl carbon atom registering at δ_C 220.1. DEPT-135 data indicate that the signal at δ_C 41.0 represents both a methine and methylene carbon atom. The five chlorine-bearing carbon atoms register at δ_C 80.8, δ_C 80.9, δ_C 104.2, δ_C 130.99, and δ_C 131.01. The signals of the olefinic carbon atoms can be distinguished from these and appear at 130.99, and δ_C 131.01. The disubstituted carbon atom (C-16) registers at δ_C 104.2. In the proton NMR spectrum the bridgehead methylene protons (H-15_a and H-15_s) register as an AX spin system at

δ_H 1.68 and δ_H 1.76 with a coupling constant of 11.28 Hz. The methylene protons H-12_a and H-12_s register as doublets at δ_H 2.21 and δ_H 2.35 with a coupling constant of 19.34 Hz. The doublet at δ_H 2.21 (H-12_s) is split due to the presence of H-13. The signal at δ_H 3.06 integrates for two protons and represents the methine protons H-3 and H-8, respectively. Six methine protons register in the complex pattern between δ_H 2.30 and δ_H 2.70.

The reaction between **1** and hexachlorocyclopentadiene (**9**) can give rise to four structural isomers, i.e. two *exo*-adducts and two *endo*-adducts (**Figure 2.2**). However, GC analysis indicated the presence of only one product. Examination of molecular models and consideration of the relative energies of the possible products showed that formation of the *exo*-adducts are unlikely. The configuration of **126** was determined by X-ray crystal structure analysis (**Figure 2.2**).

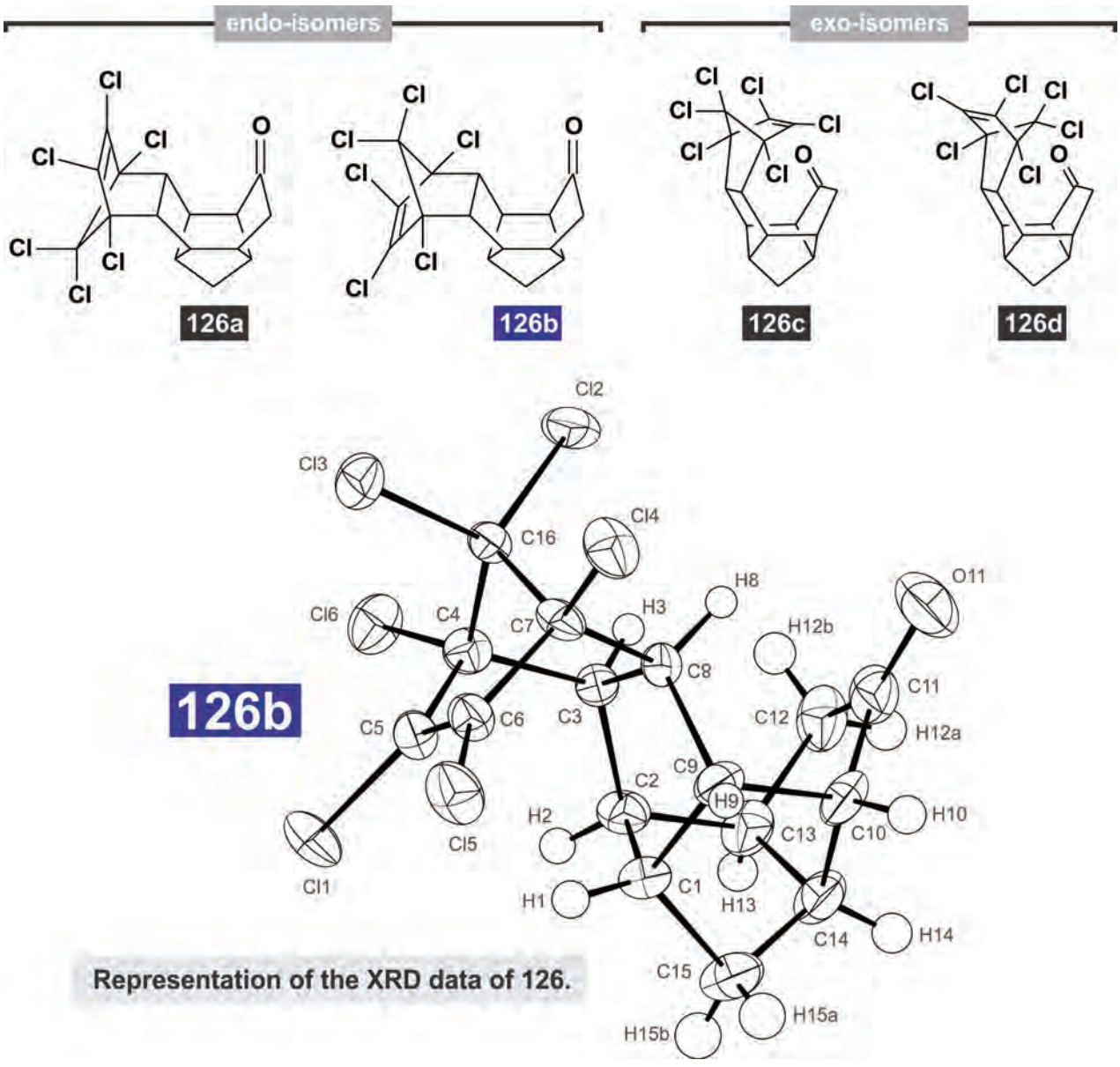

Figure 2.2: Possible isomers of **126** and the representation of the XRD data obtained.

The resolved structure showed that the ethylene bridge (C-5 and C-6) is situated on the same side as the bridgehead carbon atom (C-1). The crystallographic data are given in **Chapter 6** (➡ p. 175). To aid in the rationalisation of the experimental result, the energy profiles of the Diels-Alder reactions yielding the isomers **126a** and **126b** were determined from molecular modelling data (DFT/B3LYP/6-31G**). **Scheme 2.9** includes a representation of one of the possible transition states for the Diels-Alder reaction between the ketoalkene **1** and **9**. Transition state energies were only calculated for transition state structures that exhibited one imaginary frequency.

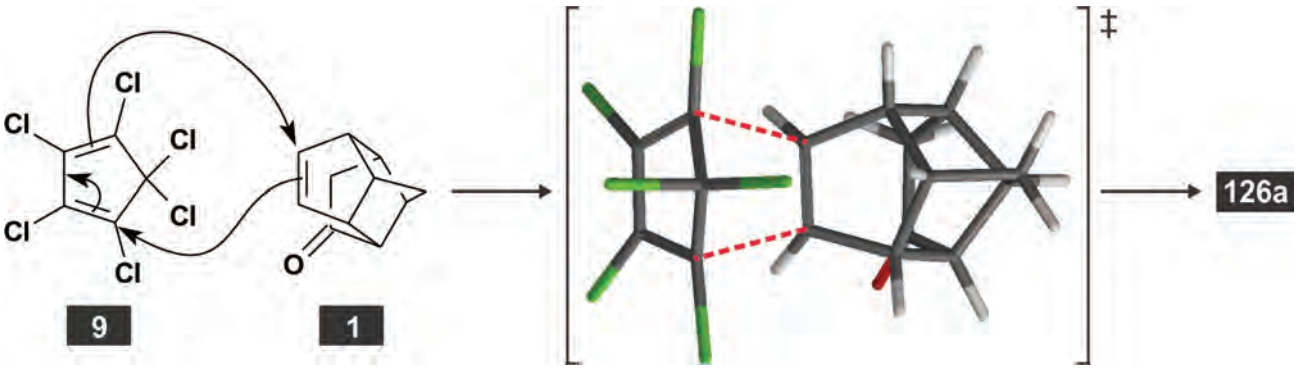

Scheme 2.9: Diels-Alder reaction between the ketoalkene **1** and **9**.

The energy profiles for the formation of **126a** and **126b** are shown in **Figure 2.3**. The profiles show that the adduct **126b** is both the kinetic and thermodynamic product of the reaction between **1** and **9**. This information is in agreement with the XRD-data.

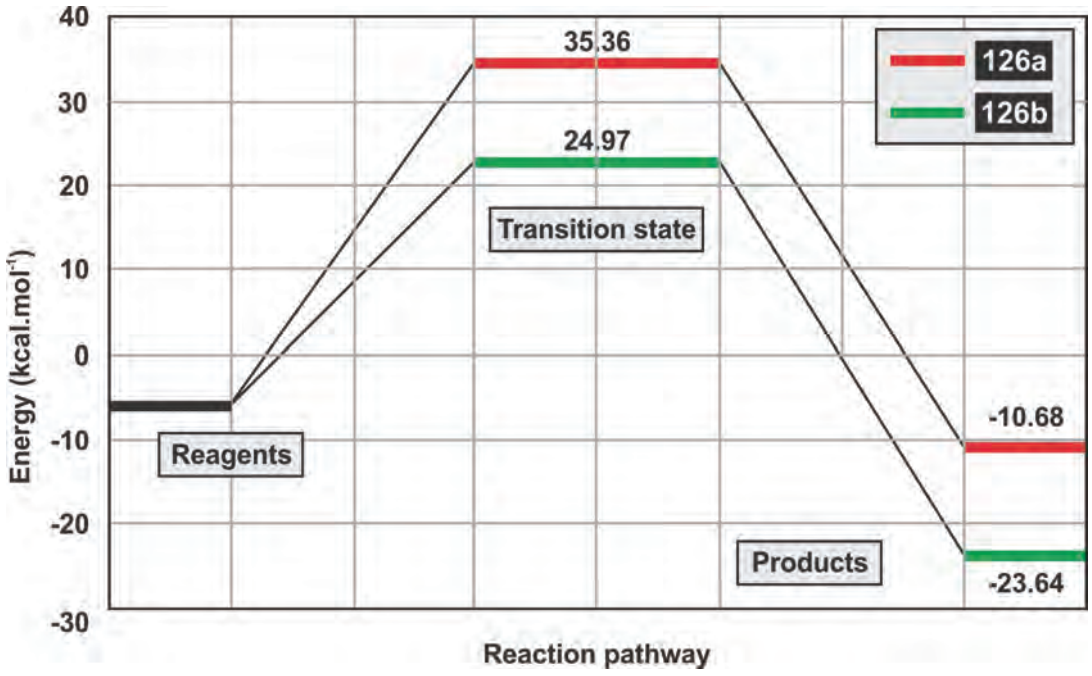

Figure 2.3: Energy profiles for the formation of **126a** and **126b**.

The Huang-Minlon modification[171-172] of the Wolff-Kishner reaction has been used routinely for decarbonylation in the preparation of cage hydrocarbons.[32,173-175] A mixture of the cage compound **126b**, hydrazine hydrate, potassium hydroxide, and diethylene glycol was refluxed for two hours. The refluxed condenser was then removed and heating continued until the temperature of the mixture reached 195°C. The mixture was kept at this temperature for 4 hours. Analysis of the reaction mixture showed that the reduction reaction removed not only the carbonyl group but also progressively removed the chlorine atoms from **126b**. To compensate for this competing reaction, an eight-fold excess of Wolff-Kishner reagent was employed. The progressive dehalogenation of **126b** led to a complex mixture of partially dehalogenated compounds. GC-MS analysis indicated that the major constituent of the mixture was a compound from which two halogen atoms and the ketone functionality had been removed. (A maximum of four chlorine atoms could be removed from **126b** when the reaction time was increased.) These products were not isolated or characterised.

Complete dehalogenation of the mixture of partially dehalogenated compounds was achieved with sodium metal and *t*-butanol in refluxing THF. Hexacyclo[7.6.1.$0^{3,8}$.$0^{2,13}$.$0^{10,14}$]hexadec-5-ene (**127**) is an oil that could be purified by distillation. The symmetry of the compound simplifies the NMR data (**Table 2.6**). Only ten signals appear in the 150 MHz ^{13}C NMR spectrum ($CDCl_3$). The olefinic carbon atoms register at 135.8 ppm. The 600 MHz ^{1}H NMR spectrum of **127** shows a prominent singlet signal at δ_H 6.03 that represents the olefinic protons (H-5 and H-6). The signals of the methylene protons register as a doublet at 1.78 ppm (H-11_a and H-12_a) and a multiplet at 1.49 ppm (H-11_s and H-12_s). The assignments of the remaining signals in the ^{1}H NMR and ^{13}C NMR spectra followed from COSY and HSQC data and are shown in **Table 2.6**. The reported geometry of **127** is based on the previously-established geometry of the adduct **126**.

Table 2.6: ^{1}H and ^{13}C NMR data[x] of 127

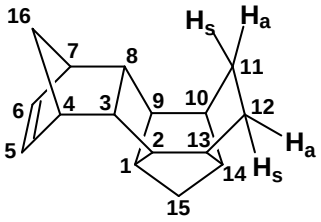

127

Number C/H	δ^{y}_{H} (ppm)	J (Hz)	δ^{y}_{C} (ppm)
1	2.58		46.5
2/9	1.66		43.8
3/8	2.57		47.3
4/7	2.69		47.4
5/6	6.03		135.8
10/13	1.99		45.0
$11_a/12_a$	1.78	8.8	25.4
$11_s/12_s$	1.49	-[z]	
14	1.99		48.7
15	1.29		30.8
16	1.36		53.6

[x] ^{1}H NMR spectrum: 600 MHz, ^{13}C NMR spectrum: 150 MHz

[y] Solvent: $CDCl_3$

[z] Coupling constant could not be determined due to overlap of these proton signals.

Two possible synthesis routes to **125** are shown in **Scheme 2.8** (➡ p. 41). The first route involves the reaction of the hydroxyalkene **118** with **9** and is followed by dehalogenation of the adduct **124**. In the second route, the adduct **126b** is reduced to **124** and then dehalogenated. Unexpectedly, neither of these routes yielded the cage alcohol **125**. **Figure 2.4** shows the energy profiles of five Diels-Alder reactions. The dimerisation of **9** has the highest activation energy of the reactions considered and is not observed in the absence of a catalyst. The exceptional reactivity of **9** in the presence of aluminium chloride has been ascribed to the formation of the pentachlorocyclopentadienyl cation ($C_5Cl_5^+$).[176] The activation energy for the dimerisation of cyclopentadiene is lower than that of the reaction between cyclopentadiene and **1**. This is a possible explanation for the observation that cyclopentadiene did not react with **1**. The transition state energy of the reaction between **118** and **9** is only marginally higher than that of the reaction between the **1** and **9**. This small difference probably does not account for the lack of reactivity of **118** towards **9**.

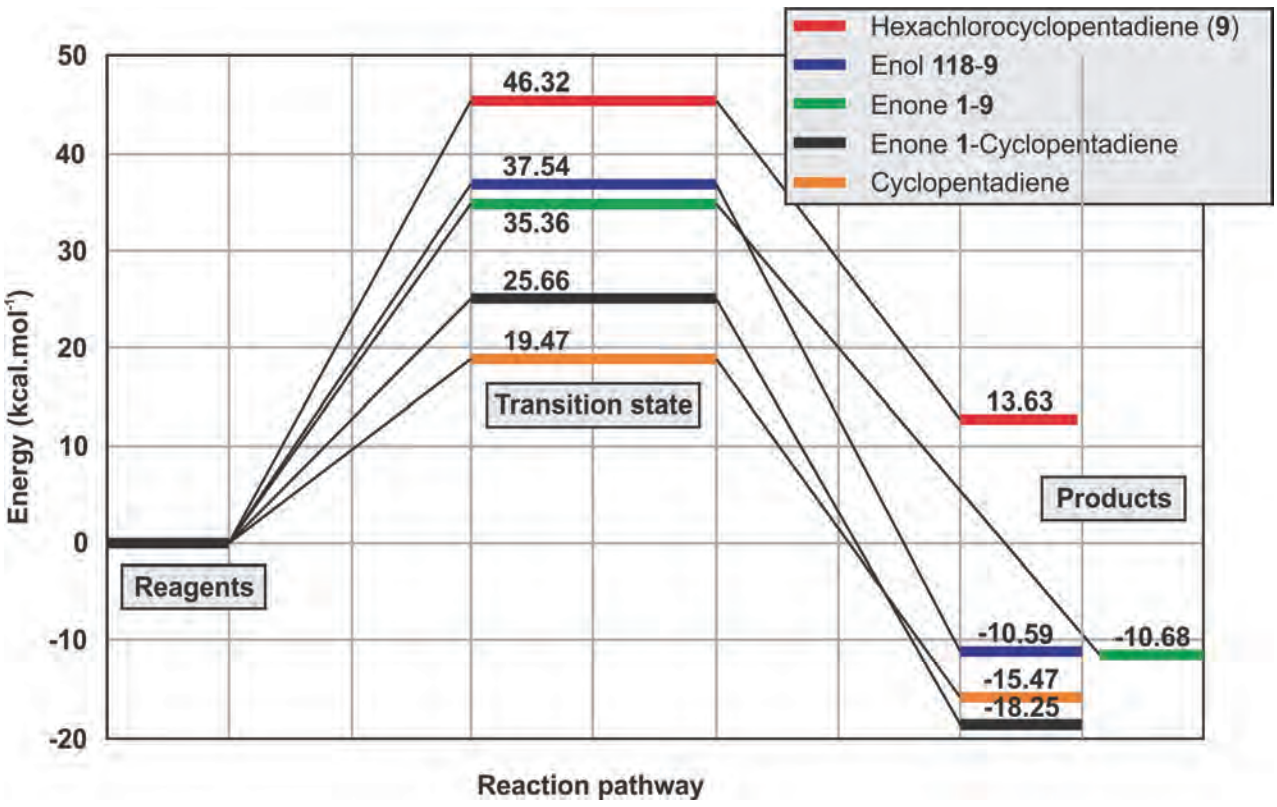

Figure 2.4: Energy profiles for the formation of different Diels-Alder adducts.

The orientation of the hydroxyl group in **118** may be a factor that influences the reactivity of the system. During a conformational search, the lowest energy orientation of the hydroxyl group was established. The lowest energy conformation has the hydroxyl group orientated towards the double bond and between the olefinic hydrogen atoms of **118** (**Figure 2.5**). This configuration may influence the reactivity of **118** towards **9** negatively. However, the rotational barrier is only about

3 kcal·mol^{-1}. Since the amount of energy available at room temperature is approximately 20 kcal·mol^{-1},[177] the hydroxyl group should rotate freely and all conformations should be accessible at and above this temperature.

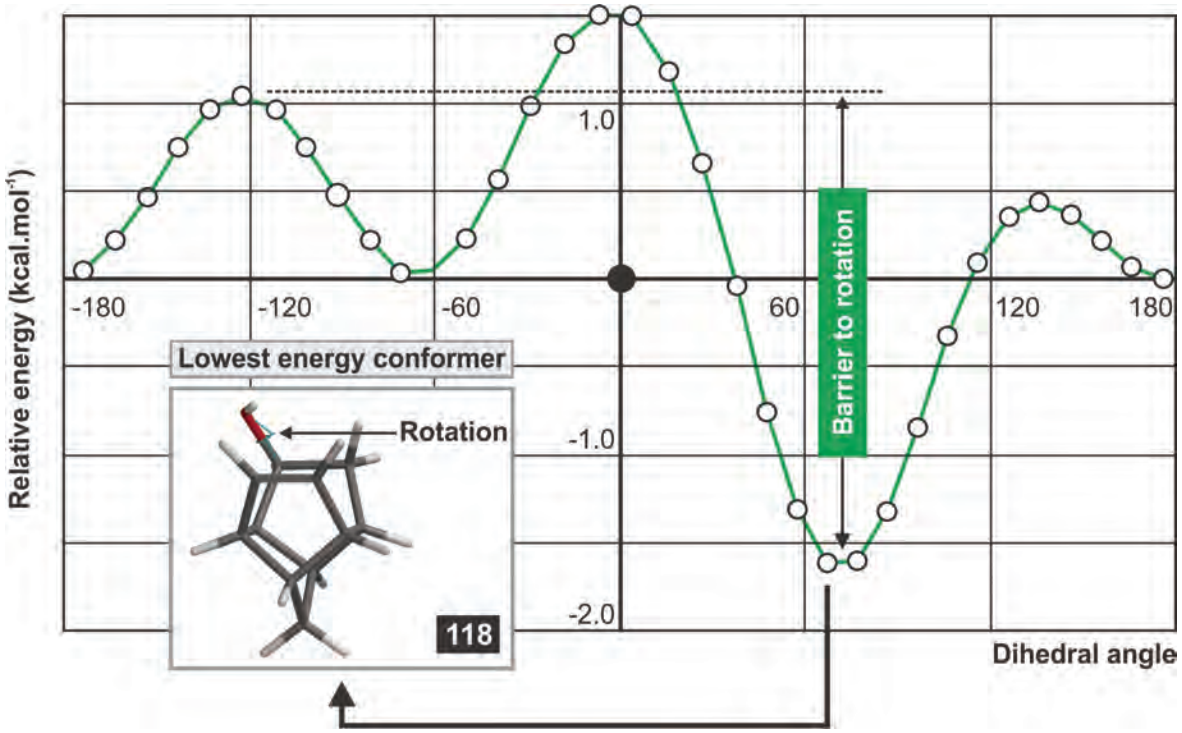

Figure 2.5: Conformation search for **119**.

A plot of the energies of the HOMOs and LUMOs of **1**, **118** and **9** indicated that the important interactions should be between the HOMOs of **1** and **118** and the LUMO of **9**. Subsequently, the shape, size and orientation of the HOMO of **118** were calculated for each of the thirty-six structures obtained from the conformation search. The data obtained were examined for anomalies, such as distortion of the HOMO by the position of the hydroxyl group. Comparisons between the results obtained for **1** and **118** did not reveal a reason for the difference in reactivity between these compounds. **Figure 2.6** shows representations of possible interaction between the HOMOs of **1** and **118** and the LUMO of **9**. On examination of these representations it should be noted that the sizes of the important HOMO and LUMO lobes are more comparable in the case of **1** and **9** than in that of **118** and **9**.

There seems to be a good correlation between the activation energy and the polar character of Diels-Alder reactions.[178] **Figure 2.7** (➡ p. 49) depicts electrostatic potential maps of **1** and **118** Comparison of these representations shows that the alkene functionality of **1** is more positive and more polarised compared to the same group in **118**. These results suggest that the reactivity of **1** should be more than the reactivity of **118** towards the same diene. Despite many attempts, the

reason for the lack of reactivity of **118** towards **9** still remained vague. It may be that the observed reactivity is the result of more than one of the above-mentioned factors.

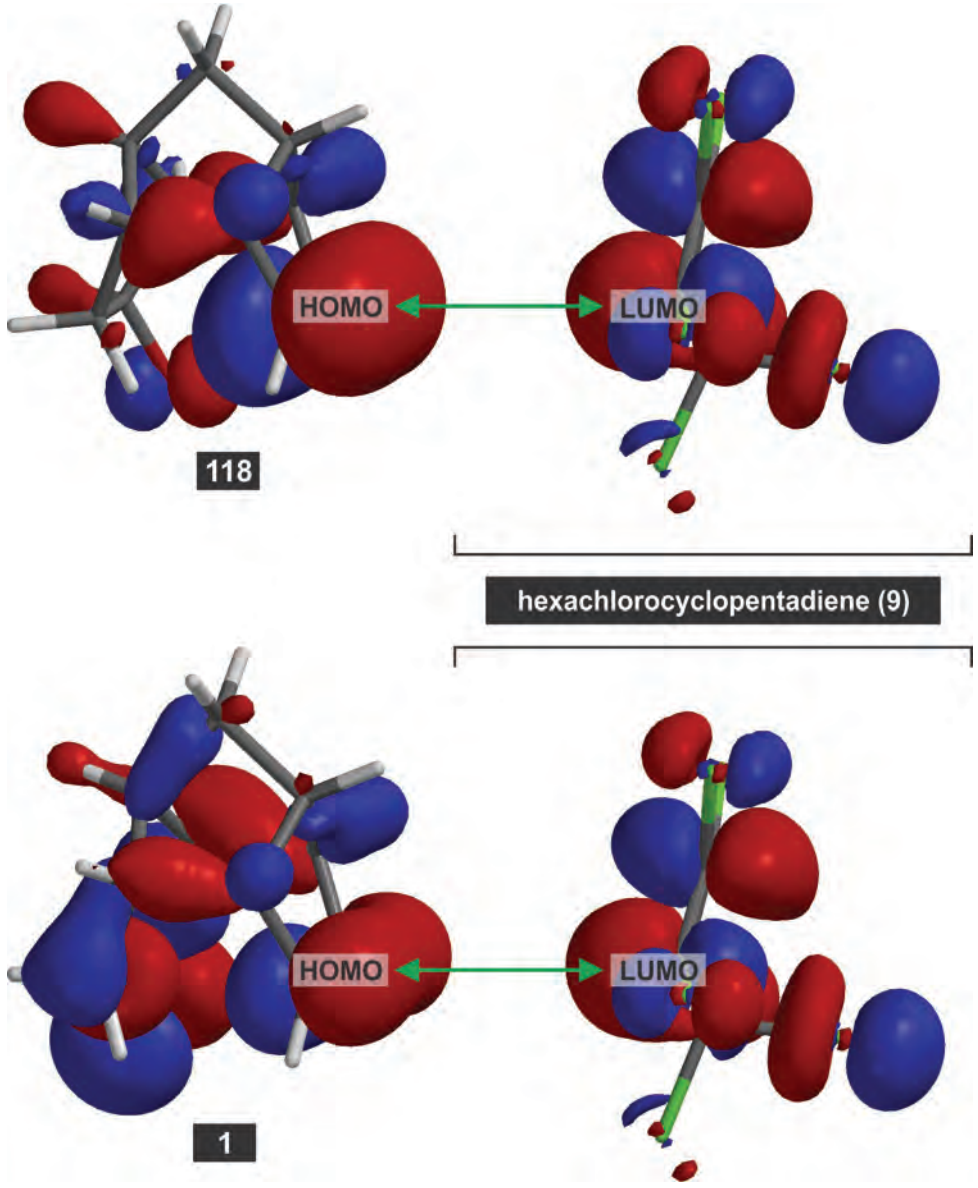

Figure 2.6: Comparison of the HOMO-LUMO interaction of **1** and **118** with **9**.

The reduction of **126b** with sodium borohydride was unsuccessful. However, it is known that the reducing ability of sodium borohydride can be enhanced by the presence of cerium(III) chloride.[179-180] The attempted reduction of **126b** was done according to the procedure of Marchand *et. al*.[12] The cage compound was dissolved in a 0.4 M solution of $CeCl_3 \cdot 7H_2O$ in methanol and cooled to 0°C. Sodium borohydride was then added in small portions at such a rate that the temperature of the reaction mixture did not rise significantly above 0°C. After addition of the $NaBH_4$, the reaction mixture was stirred at room temperature for four hours and then refluxed for 8 hours. Only starting material could be recovered from the reaction mixture.

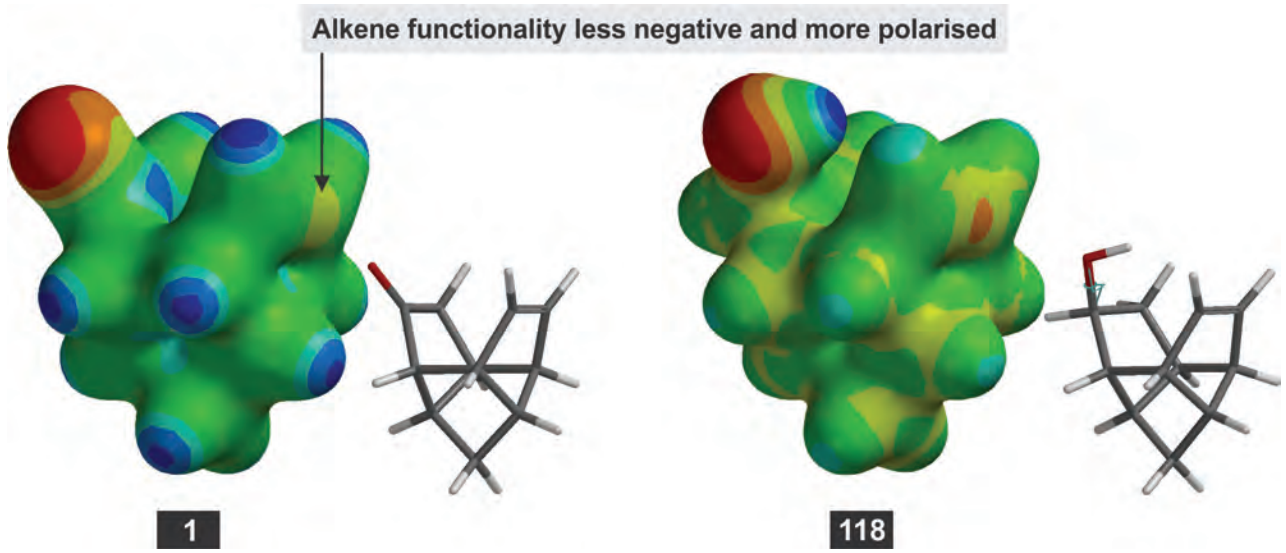

Figure 2.7: Electrostatic potential maps of **1** and **118**.

Marchand *et. al*[12] reported the reduction of the adduct **128** and the corresponding cage compound **129** (**Scheme 2.10**). Reduction of the adduct **128** with $NaBH_4$-$CeCl_3$ produced the *exo,exo*-diol **131**, while the cage compound **129** did not react under the same and more harsh reaction conditions. The similarities between compounds **128**, **129** and **126b** provided an ideal opportunity for comparison.

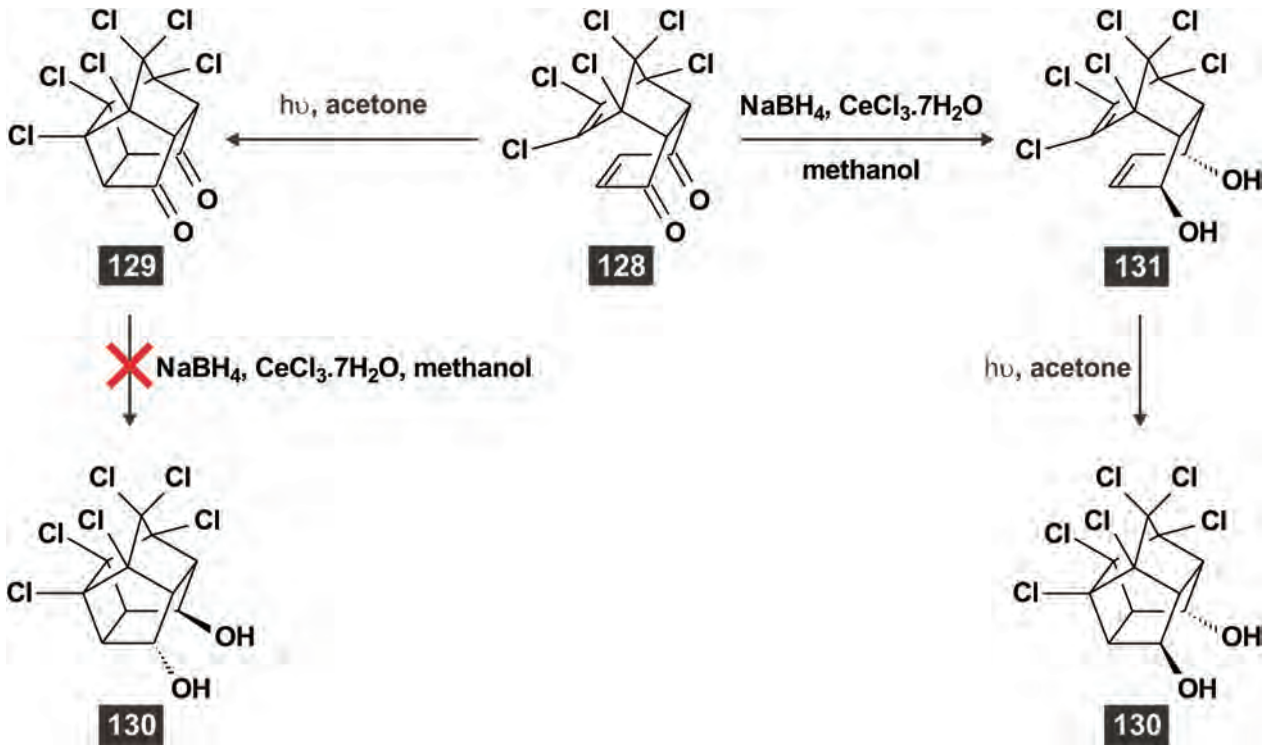

Scheme 2.10[12]**:** Reduction of ketones with $NaBH_4$-$CeCl_3$.

The reduction of a ketone with sodium borohydride involves the transfer of a hydride ion to the carbonyl carbon atom (**Scheme 2.11**).[181] The mechanism of reduction with $NaBH_4$-$CeCl_3$ is similar, with the exception that the Ce^{3+} ion catalyses the reaction between methanol and sodium borohydride to yield chemical species of the form $BH_{4-n}(OCH_3)_n$ that are stronger reducing agents than BH_4^-.[179-180] (These reducing species have increased HSAB[182]-hardness.) The Ce^{3+} ion may also complex with methanol and in doing so aid the hydrogen transfer to the carbonyl oxygen atom. During reduction of **126b** with $NaBH_4$ or $NaBH_4$-$CeCl_3$, this nucleophilic attack should be from the *exo*-face of the carbonyl group due to the steric influence of the methylene hydrogen atoms at C-12.

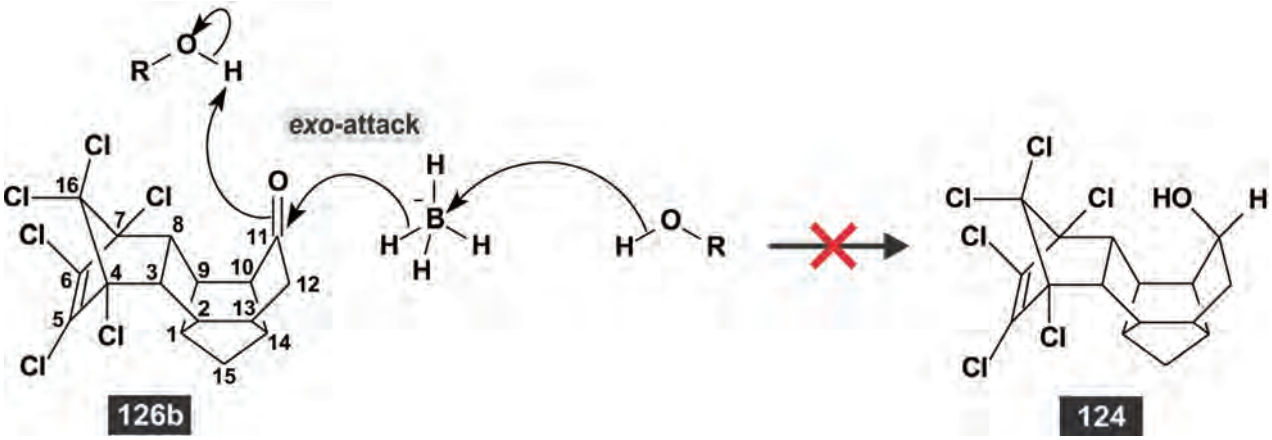

Scheme 2.11: Mechanism of reduction with sodium borohydride applied to **126b**.

Molecular modelling (DFT/B3LYP/6-31G**) was used to further investigate the lack of reaction between **126b** and sodium borohydride. **Figure 2.8** illustrates different ways in which the information obtained from the investigation can be represented. Part (a) of the figure shows the LUMO of **1**. The molecule has one LUMO with differently coloured lobes representing different phases. Part (b) of the figure shows a representation where the total electron density of **1** is superimposed on its LUMO electron density. Areas where the LUMO extends beyond the total electron density (protrudes from the total electron density) represent potential sites for nucleophilic attack.

The LUMO and SLUMO of **1**, **123**, and **126b** are compared in **Table 2.7**. The LUMO at the carbonyl carbon atom of **126b** is small compared to those observed for **1** and the simplified structure **123**. Also, the LUMO of **126b** does not extend beyond the total electron density in the region of the carbonyl group. Considering the LUMO only, it may be fair to conclude that reactions between **126b** and nucleophiles should be unlikely. In contrast, it appears possible to reduce **1** and **123** with sodium borohydride. It should be noted that the SLUMO of **126b** protrudes somewhat from the total electron density. However, the extent of this protrusion is smaller than in the cases of

3the HOMO protrusions observed for **1** and **123**. The LUMOs and SLUMOs of **128** and **129** are compared in **Table 2.8**. Neither the LUMO nor the SLUMO of **129** protrudes to any significant extent from the total electron density in the region of the carbonyl group.

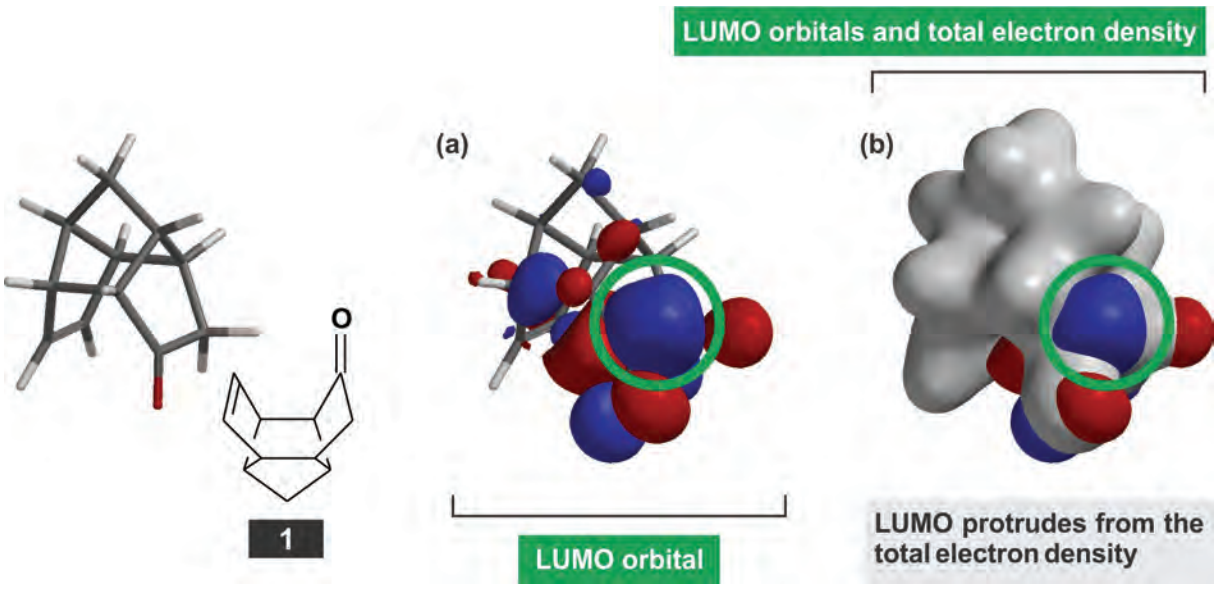

Figure 2.8: Representation of the LUMO and total electron density of **1**.

In conclusion it may be pointed out that the reactivity of ketones towards nucleophilic addition is influenced by a number of factors, including the structure of the substrate, the presence of Lewis acids, the reactivity of the nucleophile, and the stability of the tetrahedral intermediate. The fact that the adduct **128** can be reduced with $NaBH_4$-$CeCl_3$ indicate that the lack of reactivity of **126a** cannot be ascribed to the electron withdrawing effect of the chlorine atoms only. It seems likely that the presence of the PCU framework in both **126a** and **129** is a key factor in the reactivity of these compounds.

Table 2.7: Comparison of the LUMOs and total electron densities of 1, 123 and 126b

Substrate		LUMO	SLUMO	LUMO superimposed on total electron density	SLUMO superimposed on total electron density
1		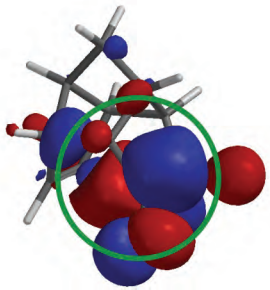	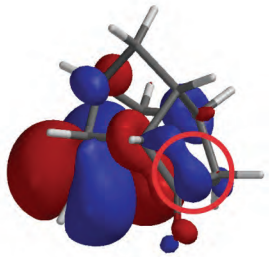	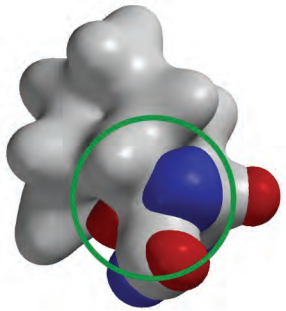	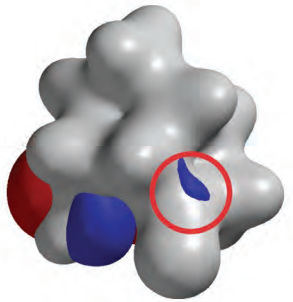
123	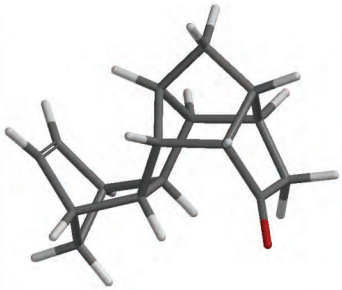	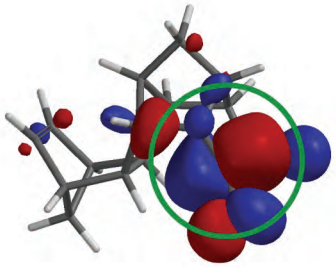	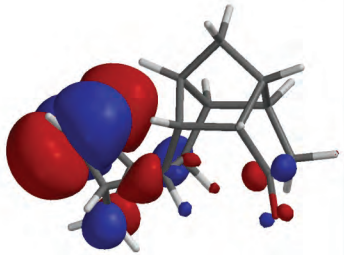	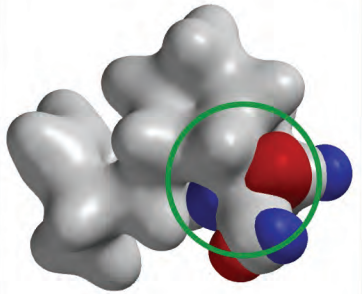	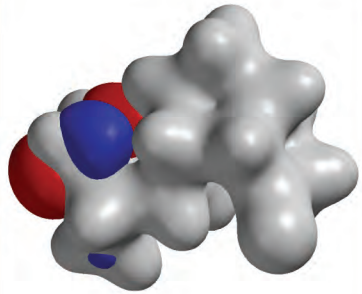
126b	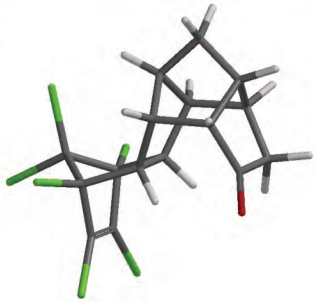	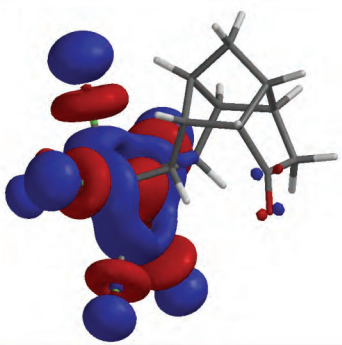	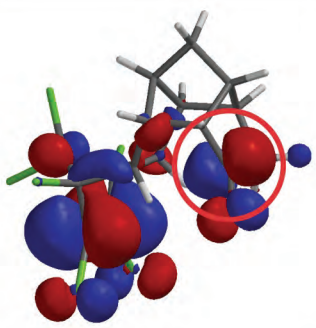	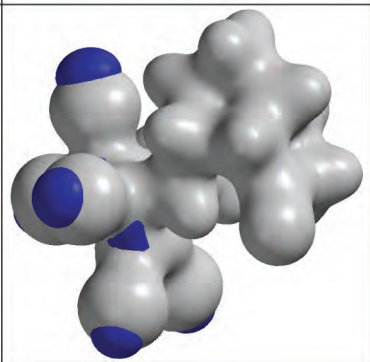	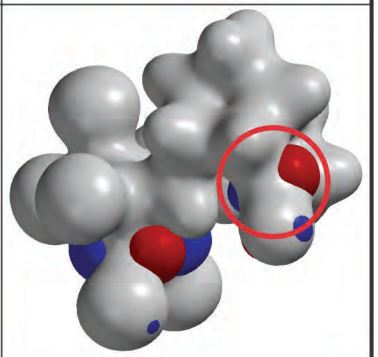

Table 2.8: LUMO, SLUMO and total electron density of 128 and 129

	Substrate	LUMO	SLUMO	LUMO superimposed on total electron density	SLUMO superimposed on total electron density
128	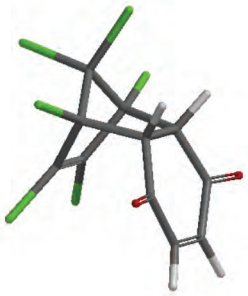	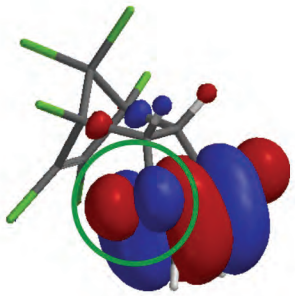	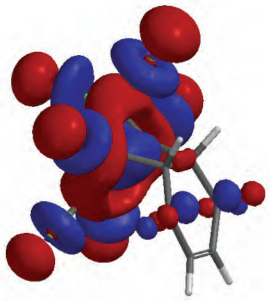	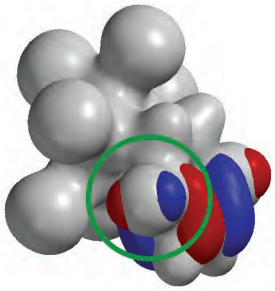	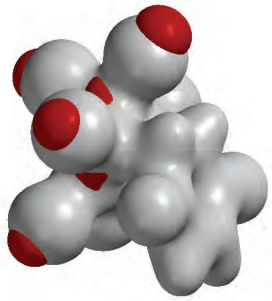
129		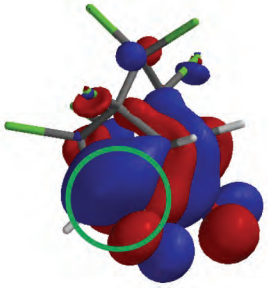	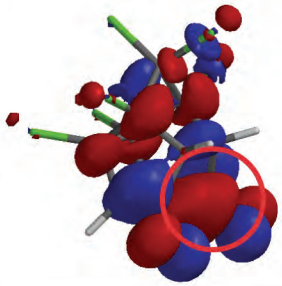	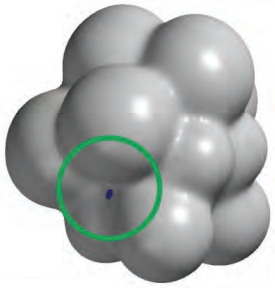	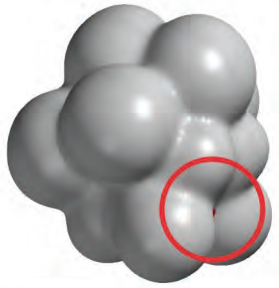

2.3. Synthesis of derivatives of 4-isopropylidenepentacyclo[5.4.0.0^{2,6}.0^{3,10}.0^{5,9}]-undecane-8,11-dione

Attempts to synthesise a new cage alkene **136** are described in this section. The selected synthetic route should either conserve the alkylidene group at the bridgehead or make provision for its later reintroduction. In this study the former approach was selected. An outline of the synthesis strategy is given in **Scheme 2.12**.

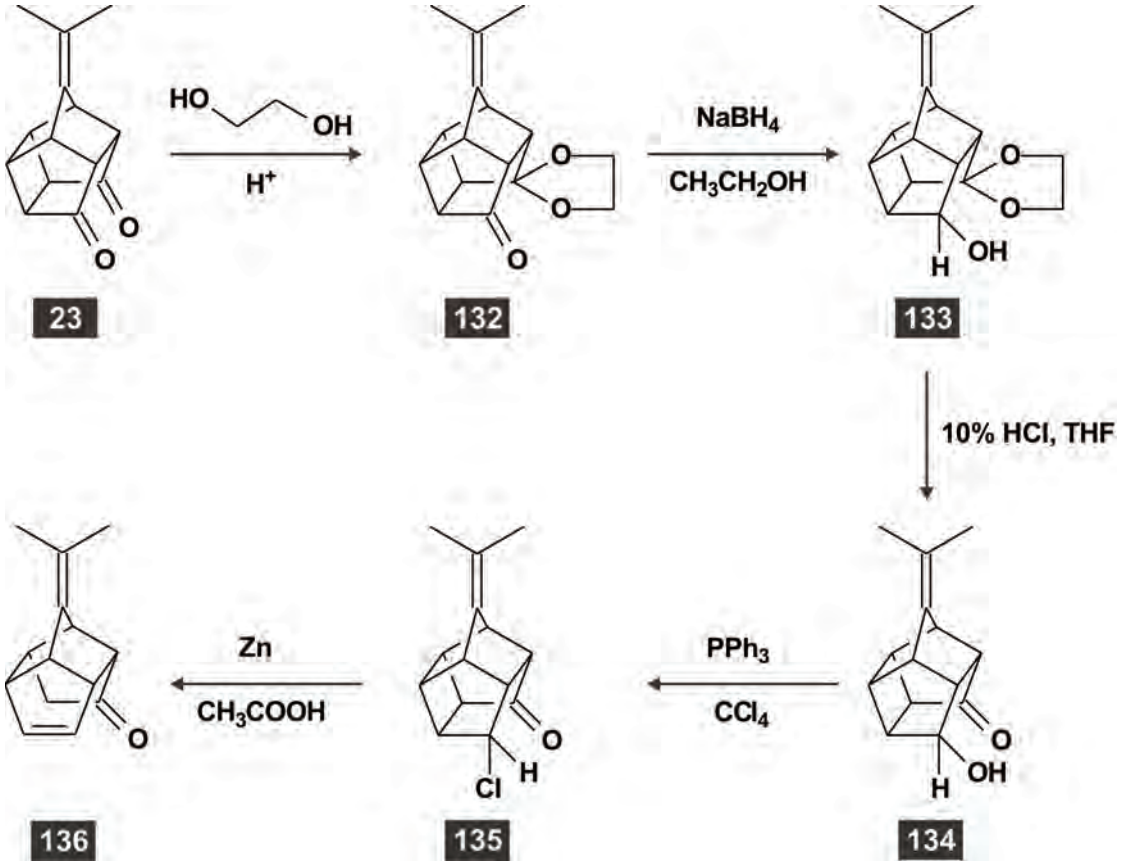

Scheme 2.12: Synthesis of 10-isopropylidenetetracyclo[6.3.0·0^{4,11}.0^{5,9}]undec-2-en-6-one.

Isopropylidenepentacyclo[5.4.0.0^{2,6}.0^{3,10}.0^{5,9}]undecane-8,11-dione[183] (**23**) was used as the starting material in this study. This compound is the product of the photocyclisation of the *endo*-adduct **22b** of 1,4-benzoquinone (**11**) and 6,6-dimethylfulvene (**21, Scheme 2.12**). In a very similar system, the cycloaddition of 1,4-benzoquinone (**11**) to 1,3-cyclopentadiene leads predominantly to the *endo*-product **41** (➡ p. 9).[184] In contrast, Griesbeck[185] reported that the reaction of **11** and **21** produced approximately a 1:1 ratio of *exo*-adduct **22a** and *endo*-adduct **22b** in a representative selection of non-aqueous solvents (**Scheme 2.13**). Extended reaction times favoured the formation of the *exo*-adduct (thermodynamic product).[186] Conducting the reaction in a polar solvent increased the reaction rate and favoured the kinetically-favoured *endo*-adduct **22b**.[183,185]

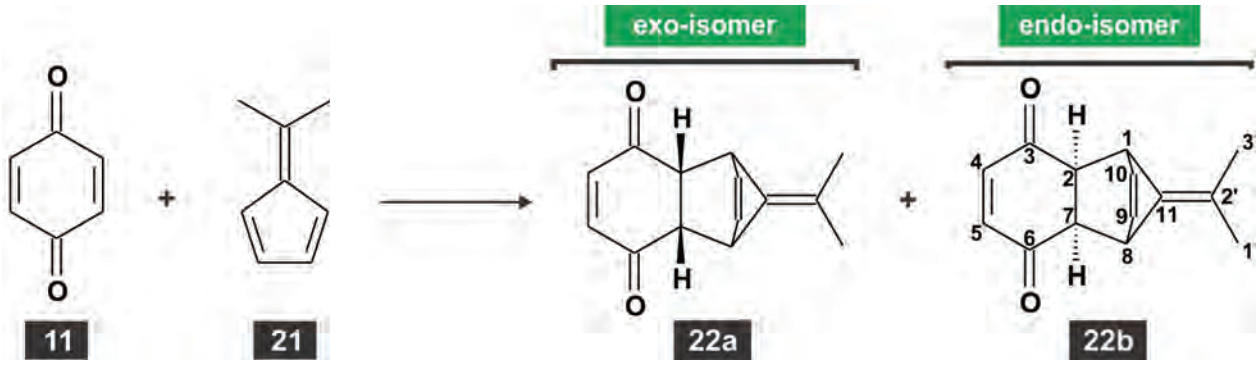

Scheme 2.13[187]**:** Synthesis of 11-(propan-2-ylidene)tricyclo[6.2.1.0^{2,7}]undeca-4,9-diene-3,6-dione.

The energy diagram in **Figure 2.9** shows that the energy of the *exo*-adduct **22a** is lower than that of the *endo*-adduct **22b**. However, the energy of the transition state of **22b** is lower than the energy of the transition state of **22a**. These results indicate that it should be possible to obtain the *endo*-adduct through kinetic control of the reaction. This conclusion from the energy diagram is in agreement with the experimental result.

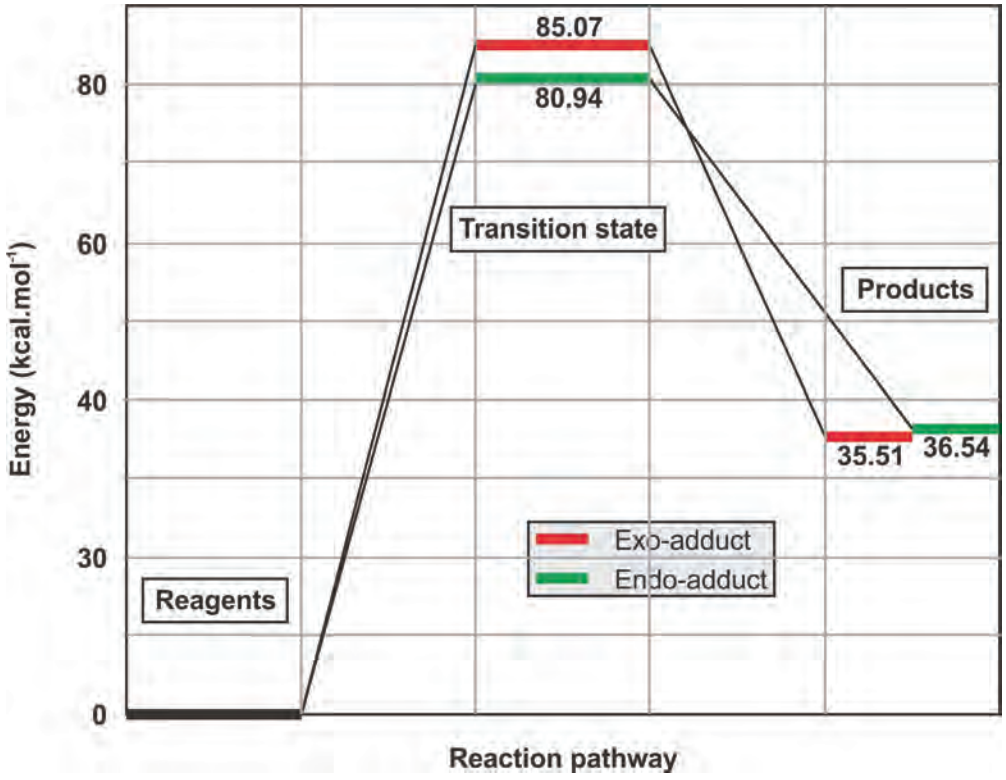

Figure 2.9: Energies for the cycloaddition of 1,4-benzoquinone (**11**) to 6,6-dimethylfulvene (**21**).

Griesbeck[187] showed that using water as solvent significantly influenced both the rate and stereoselectivity of the reaction between **11** and **21**. The rate of the reaction increased by a factor of up to 100 compared to the rate in aprotic organic solvents and by a factor of 20 – 40 compared

to the rate in protic organic solvents.[187] Using water as solvent significantly increased the stereoselectivity of the reaction in favour of the *endo*-adduct **22b** (**Table 2.9**).

Table 2.9[187]: Reaction of 6,6-dimethylfulvene and 1,4-benzoquinone in water

C^{x} fulvene (mol·dm^{-3})	C^{x} benzoquinone (mol·dm^{-3})	Reaction time (h)	Ratio 22a: 22b
0.001	0.001	24	88: 14
0.019	0.019	16	77: 23
0.019	0.038	16	62: 38
0.090	0.090	12	60: 40
0.090	0.180	12	41: 59
0.472	0.472	8	24: 76
1.600	1.600	8	12: 88

[x] Formal concentrations are given rather than actual concentrations due to the poor solubilities of reagents in water.

Rate enhancements by a factor of up to 700 have been reported for cycloaddition reactions when the solvent was changed to water.[188-192] Reactions of organic reagents in water are frequently biphasic and water may not be acting as a traditional solvent. The rates of heterogeneous aqueous reactions are often proportional to the speed and method of mixing and inversely proportional to the reaction temperature.[193] Rate enhancements in aqueous media have been ascribed to the hydrophobic effect.[194] Other explanations consider factors such as the cohesive energy density of the aqueous media, increased hydrogen bonding in the transition state, and a decrease in the volume of the transition state in some reactions.[193] Consensus regarding the explanation for the rate enhancements of aqueous heterogeneous reactions has not been reached yet.

The *endo*-adduct **22b** was initially synthesised according to the method of Griesbeck.[183] High formal concentrations of 1,4-benzoquinone (**11**) and 6,6-dimethylfulvene (**21**) were stirred mechanically in water for a period of 12 hours during which time a solid product formed. The reaction was conducted at room temperature due to the fast retro cleavage observed at higher temperatures.[185] Although the desired product was obtained from this procedure, substantial amounts of 1,4-benzoquinone and unreacted 6,6-dimethylfulvene were detected. The 1,4-hydroquinone was formed by the reduction of 1,4-benzoquinone.[195] Purifying the product was tedious and a yield of only 60% could be realised. Remarkably, it was found that conducting the cycloaddition without solvent consistently produced results similar to that found with high formal reagent concentrations in water. The reaction produced a 77% yield of the *endo*-adduct **22b** – in excellent agreement with the 81% yield reported by Griesbeck.[183] Conducting the reaction without solvent yielded a much cleaner product than the conventional method.

The *endo*-adduct **22b** undergoes relative fast cycloreversion in organic solvents at room temperature when compared to the adduct **41**.[185] This can probably be ascribed to the abnormally small bonding angle caused by the presence of the sp^2-hybridised carbon atom at the bridgehead (C-11, compound **22b**, **Scheme 2.13**). Molecular modelling (DFT/B3LYP/6-31G**) puts the size of the C_1-C_{11}-C_8 angle at 95.83°, compared to a value of 102.95° in cyclopentane. The presence of the sp^2-hybridised carbon atom at C-11 also flattens the five-membered ring fragment slightly and increases torsional strain relative to cyclopentane. Upon ultraviolet irradiation, more rapid decomposition of **22b** was observed resulting in the formation of a black tar. The tar contained 6,6-dimethylfulvene, hydroquinone (from 1,4-benzoquinone) and unidentified polymeric products. Due to the instability of **22b** during irradiation, a systematic search was conducted to identify the optimum concentration and irradiation duration for the available infrastructure. The maximum yield of 40% of **23** was achieved by irradiation of 500 mg of **22b** in 50 cm^3 acetone for two hours. Griesbeck[183] reported a 88% yield of **23** when using a falling film photoreactor. Without this apparatus, yields higher than 40% are improbable.

The IR spectrum of **23** exhibits a strong carbonyl group absorption at 1728 cm^{-1}. The mass spectrum shows a molecular ion at *m/z* 214 that supports a molecular formula of $C_{14}H_{14}O_2$. The NMR spectra of dimethylfulvene cage compounds are simpler than those of the corresponding PCU derivatives. The 150 MHz ^{13}C NMR spectrum of **23** shows eight signals. The number of signals is an indication of the symmetrical nature of the compound. The absence of the signals at δ_C 121.9, δ_C 140.2, and δ_C 212.1 in the DEPT-135 spectrum indicates the presence of three quaternary carbon atoms in the structure of **23**. The alkene carbon atoms of the propylidene fragment occur at δ_C 121.9, (C-2') and δ_C 140.2 (C-4), while the carbonyl group (C-8/C-11) registers at δ_C 212.1. The signal at δ_C 21.3 represents two methyl groups (C-1' and C-3'). The 600 MHz ^1H NMR spectrum of **23** shows five singlets that integrate for a total of fourteen protons. The singlet at δ_H 1.73 integrates for six protons and represents two methyl groups (H-1' and H-3'). The assignments of the four methine signals in the ^1H NMR and ^{13}C NMR spectra of **23** followed from COSY and HSQC data and are shown in **Table 2.10**.

The reaction of **23** with ethylene glycol in the presence of a catalytic amount of PTS yielded the mono ketal **132**. The ketal functionality served as a protecting group to facilitate formation of the ketol **134a** (**Scheme 2.12**). The yield of **132** was maximised by removal of water from the equilibrium mixture. The reaction was initially conducted in benzene, but better yields were obtained using higher boiling toluene. Yields of 81% and 86 – 93% were obtained in benzene and toluene, respectively.

Table 2.10: ^{1}H and ^{13}C NMR data[x] of 23

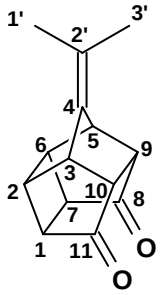

23

Number C/H	δ^{y}_{H} (ppm)	J (Hz)	δ^{y}_{C} (ppm)
1/7	3.16	-	38.1
2/6	3.25	-	43.2
3/5	2.69	-	53.5
4	-	-	140.2
8/11	-	-	212.1
9/10	2.81	-	44.4
1'/3'	1.73	-	21.3
2'	-	-	121.9

[x] ^{1}H NMR spectrum: 600 MHz, ^{13}C NMR spectrum: 150 MHz

[y] Solvent: $CDCl_3$

The IR spectrum of **132** exhibits a carbonyl group absorption at 1734 cm^{-1} and a complex pattern[196] at 1104 cm^{-1}. Support for a molecular formula of $C_{16}H_{18}O_3$ is derived from the mass spectrum, which shows a molecular ion at *m/z* 258. Possible assignments of the resonance signals in the ^{1}H NMR and ^{13}C NMR spectra of **132** are given in **Table 2.11**.

Table 2.11: ^{1}H and ^{13}C NMR data[x] of 132

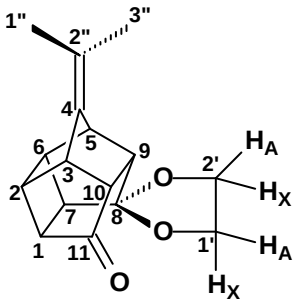

132

Number C/H	δ^{y}_{H} (ppm)	J (Hz)	δ^{y}_{C} (ppm)
1	2.61	-	41.4
2	2.86	-	35.6
3	2.98	-	41.7
4	-	-	140.4
5	3.19	-	44.8
6	3.01	-	40.8
7	2.70	-	43.2
8	-	-	113.9
9	2.52	-	52.1
10	2.50	-	49.9
11	-	-	215.1
$1'_A$	3.96[a]	-[z]	64.6
$1'_X$	3.88[a]	-[z]	
$2'_A$	3.96	-[z]	65.7
$2'_X$	3.96	-[z]	
1"	1.70[b]	-	20.99
2"	-	-	119.7
3"	1.72[b]	-	21.02

[x] ^{1}H NMR spectrum: 600 MHz, ^{13}C NMR spectrum: 150 MHz

[y] Solvent: $CDCl_3$

[z] Coupling constant could not be determined due to overlap of these proton signals.

[a, b] Values for ^{1}H NMR and ^{13}C NMR signals can be switched.

The 150 MHz ^{13}C NMR spectrum ($CDCl_3$) of **132** shows signals that may be associated with sixteen different carbon atoms. The signals at δ_C 113.9, δ_C 119.7, δ_C 140.4, and δ_C 215.1 represent quaternary carbon atoms. Comparison of the ^{13}C NMR spectra of **132** and **23** indicates that the signal at 113.9 may be assigned to the carbon atom bearing the ketal functionality (C-8). The signals at δ_C 20.99 and δ_C 21.01 represent the methyl groups (C-1'' and C-3'') in the propylidene moiety. The 600 MHz ^1H NMR spectrum ($CDCl_3$) of **132** shows two singlets that may be associated with the methyl groups attached to C-2''. The methylene protons of C-1' and C-2' register as multiplets at 3.88 ppm and 3.96 ppm. The methine protons register between δ_H 2.47 and δ_H 3.21 and integrate for eight protons. The methylene carbon atoms of the ketal group (C-1' and C-2') register at 64.6 ppm and 65.7 ppm. The HSQC spectrum of **132** shows that the protons attached to C-1' experience a larger non-equivalence shift than the protons attached to C-2'. The larger difference in chemical shift between H-1'$_A$ and H-1'$_X$ has been ascribed to through-space deshielding from the oxygen atom attached to C-11.[197-198] Examination of molecular models shows that pseudo-rotation around the C-1'-C-2' bond leads to two possible conformations for the ketal group. These structures were geometrically optimised (DFT/B3LYP/6-31G**) and are represented in **Figure 2.10**. The energy of **Conformation 1** is only about 0.1 kcal·mol^{-1} lower than that of **Conformation 2**. Since this energy difference is small, both conformations should exist at room temperature. Examination of the optimised model of **Conformation 1** reveals that H-1'$_A$ is in close proximity to H-9 and H-2'$_X$ to H-7. The situation is reversed for **Conformation 2** with H-1'$_X$ being in close proximity to H-7 and H-2'$_A$ to H-9. The NOESY spectrum of **132** should therefore show the correlations of H-1'$_X$ and H-2'$_X$ with H-7 and also the correlations of H-1'$_A$ and H-2'$_A$ with H-9. The observations in this system are similar to that observed by Kruger and Ramdhani.[197] The NOESY spectrum of **132** is shown in the spectral data section (➡ p. 160).

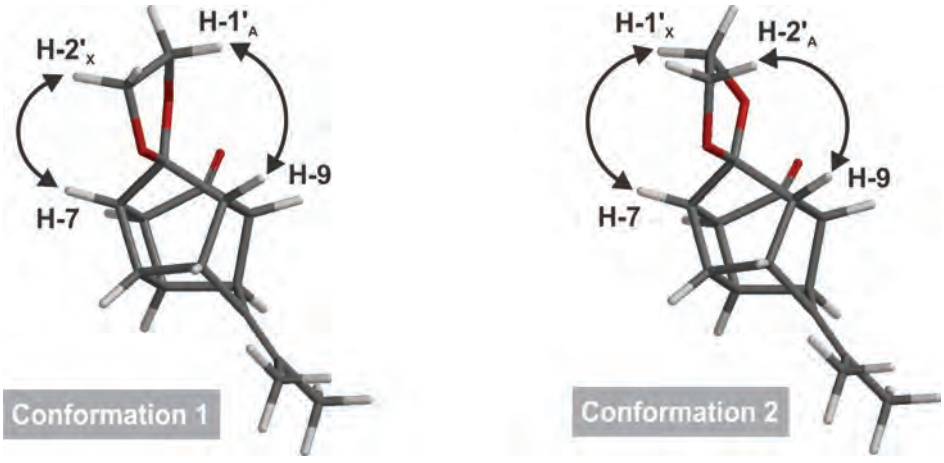

Figure 2.10: Expected NOESY interactions in **132**.

Sodium borohydride reduction of **132** produced the cage alcohol **133**. Since the solubility of **132** in ethanol is low, reduction was achieved in a mixture of THF and ethanol. THF was generally an efficient solvent for derivatives of **23**. The IR spectrum of **133** exhibits the expected O–H stretch vibration at 3428 cm^{-1}. The mass spectrum shows a molecular ion at *m/z* 260 that supports a molecular formula of $C_{16}H_{20}O_3$. The 150 MHz ^{13}C NMR spectrum ($CDCl_3$) of **133** shows signals that may be associated with sixteen different carbon atoms. The methine carbon atom bearing the hydroxyl group (C-11) registers at δ_C 72.7. The 600 MHz ^1H NMR spectrum ($CDCl_3$) of **133** shows a doublet at δ_H 5.34 that represents the hydroxyl proton. The presence of the doublet is an indication of the close proximity of the oxygen atom in the ketal moiety. The assignments of the remaining signals in the ^1H NMR and ^{13}C NMR spectra followed from COSY and HSQC data and are shown in **Table 2.12**.

Table 2.12: ^1H and ^{13}C NMR data[x] of 133

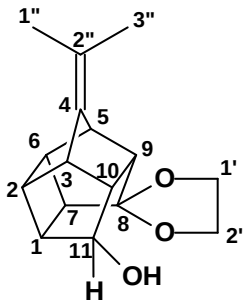

133

Number C/H	δ^y_H (ppm)	J (Hz)	δ^y_C (ppm)
1	2.72	-	39.0
2	2.57	-	38.4
3	2.68	-	42.7
4	-	-	139.1
5	2.89	-	43.6
6	2.67	-	39.2
7	2.48	-	46.8
8	-	-	115.7
9	2.24	-	46.4
10	2.48	-	39.3
11	3.65 and 3.63	12.2	72.7
1'/2'	3.93 and 3.86	43.3	63.0
2'/1'	4.00	-	65.6
1"/3"	1.65	-	20.7
2"	-	-	117.4
3"/1"	1.63	-	20.8
OH	5.35 and 5.33	12.2	-

[x] ^1H NMR spectrum: 600 MHz, ^{13}C NMR spectrum: 150 MHz

[y] Solvent: $CDCl_3$

Acid hydrolysis[199] of **133** was achieved by refluxing the compound in aqueous THF with a catalytic amount of PTS. The IR spectrum of the material obtained shows absorptions at 1717 cm^{-1} and

3259 cm^{-1} that indicate the presence of a carbonyl group and hydroxyl group, respectively. The strong absorptions at 1344 cm^{-1} and 989 cm^{-1} may be indicative of an ether grouping. Data from a GC-MS analysis of the reaction mixture indicate the presence of a single product. The MS spectrum of this product shows a molecular ion at *m/z* 216 that supports a molecular formula of $C_{14}H_{16}O_2$. In contrast, the 150 MHz ^{13}C NMR spectrum ($CDCl_3$) of the isolated product shows twenty-eight signals that indicates the presence of two isomers. The pattern of the signals in the150 MHz ^{13}C NMR spectrum indicates structural similarity between the two products, with the notable exception of the signals at δ_C 219.1 and δ_C 115.8. The signal at δ_C 219.1 represents a carbonyl carbon atom and the signal at δ_C 115.8 is that of a quaternary carbon atom bearing an electronegative group. These deductions support the conclusion that the ketol **134a** is in equilibrium with the hemiketal **134b** (**Scheme 2.14**).

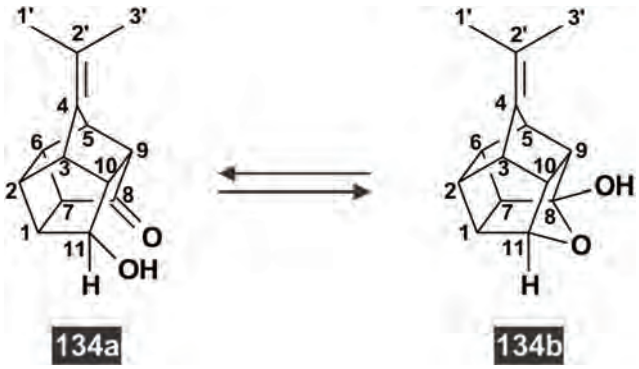

Scheme 2.14: Equilibrium between the ketol **134a** and hemiketal **134b**.

A similar equilibrium has been reported for the closely-related PCU system.[200] Transannular reactions are common in the PCU system and has been thoroughly investigated.[147] Molecular modelling (DFT/B3LYP/6-31G**) results indicate that the distance between the carbonyl carbon atoms in **23** (2.632 Å) is similar to the corresponding distance in **44** (2.635 Å). Based on these results, it seems likely for **23** and its derivatives to participate in transannular reactions.

Synthesis of *exo*-11-chloro-4-isopropylidenepentacyclo[5.4.0.$0^{2,6}$.$0^{3,10}$.$0^{5,9}$]undecane-8-one (**135**) proved much more difficult than expected. The Appel reaction was initially selected for conversion of **134a/134b** to **135** (**Scheme 2.12**). The reaction is reputed to proceed with high conversion, without rearrangement and mostly with inversion of configuration.[201] In addition, this method has been shown to transform 1-adamantanol (**137**) to 1-chloroadamantane (**138**, **Scheme 2.15**).[202]

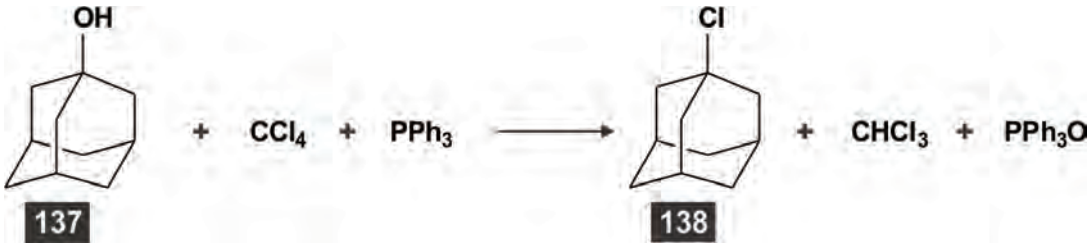

Scheme 2.15[202]**:** Conversion of 2-adamantanol to 2-chloroadamantane.

Removal of triphenylphosphine oxide was expected to be a problem during the synthesis of **135**. The conventional removal method exploits the low solubility of the oxide in pentane.[203] However, this strategy was not useful due to the equally low solubility of **134a/134b** in this solvent. Additional approaches were developed to aid in the removal of triphenylphosphine and triphenylphosphine oxide. Derivatisation of the phenyl rings of triphenylphosphine with sulphonic acid groups facilitates the formation of a water-soluble salt during extraction with basic solution.[204] Another approach utilises a resin that act as a solid support for attachment of the triphenylphosphine reagent.[202] Finally, triphenylphosphine and triphenylphosphine oxide may be removed after the reaction by the addition of a resin that acts as a scavenger.[205] The latter two strategies facilitate removal of triphenylphosphine and triphenylphosphine oxide from the product mixture by filtration.

A mixture of **134a/134b**, triphenylphosphine and carbon tetrachloride was refluxed in THF for 24 hours. Throughout this period, the reaction was monitored with GC-MS. No conversion of **134a/134b** to **135** could be detected. Most of the triphenylphosphine was converted to triphenylphosphine oxide during the reaction period, but no chloroform could be detected at any time. Subsequently, the Appel reaction was applied to a selection of cage alcohols to probe the scope of the reaction. The results of these experiments are summarised in **Table 2.13**.

Table 2.13: Summary of the Appel reaction of selected cage alcohols

Substrate	Reagents	Conditions	Result	Ref.
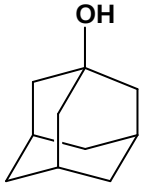 **137**	PPh_3 and CCl_4	Reflux in DCM, 18 hours.	91%	[202]

Table 2.13 - Continued

Substrate	Reagents	Conditions	Result	Ref.
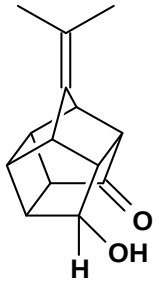 **134a/134b**	PPh_3 and CCl_4	Reflux in THF, 1 – 24 hours	No conversion	-
	PPh_3 and CBr_4	Reflux in THF, 1 – 24 hours	No conversion	-
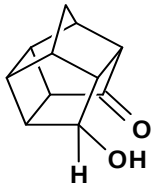 **139**[200]	PPh_3 and CCl_4	Reflux in THF, 1 – 24 hours	No conversion	-
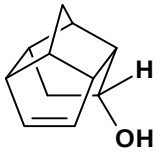 **118**[51]	PPh_3 and CCl_4	Reflux in THF, 1 – 24 hours	No conversion	-
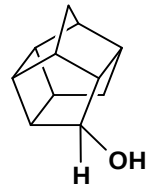 **140**[200]	PPh_3 and CCl_4	Reflux in THF, 1 – 24 hours	No conversion	-

Table 2.14 shows some calculated electronic properties (DFT/B3LYP/6-31G**) of the substrates presented in **Table 2.13**. Since the size of the HOMO and NHOMO on the hydroxyl oxygen atom varies with dihedral angle, the hydroxyl group of each substrate was subjected to a conformational search. For each substrate the conformer with the largest HOMO electron density on the hydroxyl group is shown in **Table 2.14**. The rotational barriers of these substrates are small (~ 3 kcal·mol^{-1}) and all conformations should thus be available at room temperature.

The results seem to suggest that the Appel reaction is not a suitable method for the transformation of cage alcohols to halogen compounds. The mechanism[201,206-207] of the Appel reaction is summarised in **Scheme 2.16**. The formation of the ion pair **141** is the same irrespective of the substrate used. In contrast, formation of the intermediate **142** involves a nucleophilic attack of the alcohol on the phosphorus atom and should be influenced by the electronic properties of the alcohol.

Table 2.14: HOMO, NHUMO and total electron densities of selected cage alcohols

Substrate		HOMO	NHOMO	HOMO superimposed on total electron density	NHOMO superimposed on total electron density
137		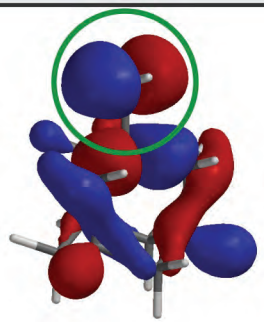	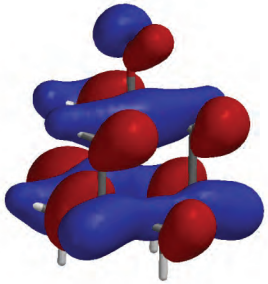	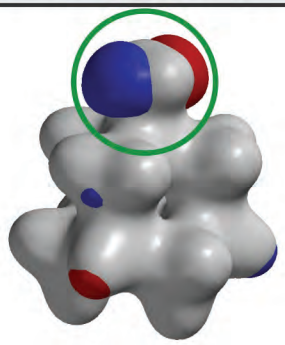	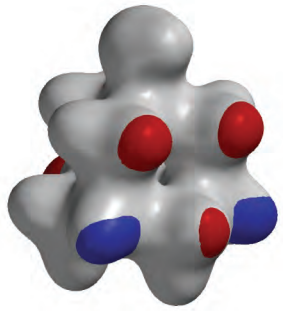
134a		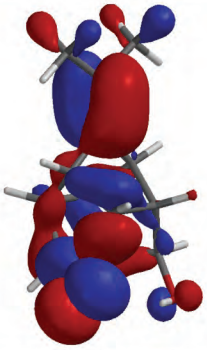	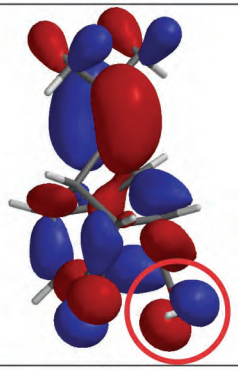	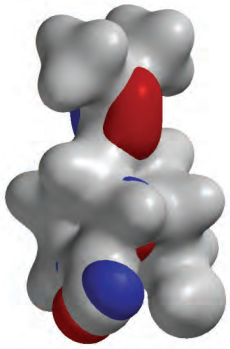	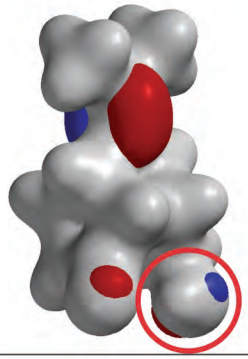
134b	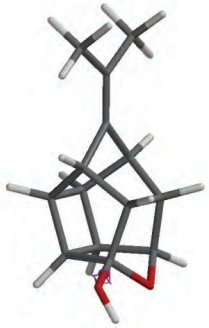	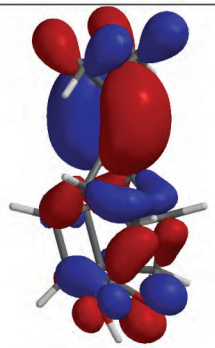	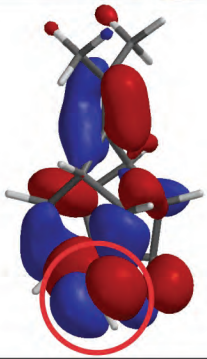	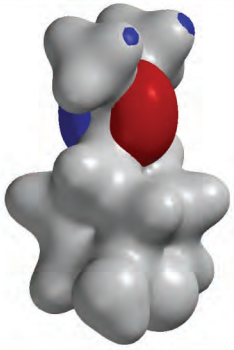	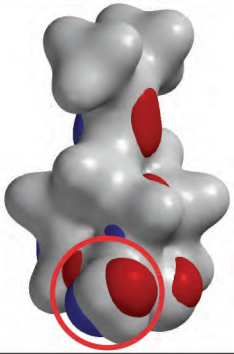

Table 2.14: HOMO, NHUMO and total electron densities of selected cage alcohols (Continued)

	Substrate	HOMO	NHOMO	HOMO superimposed on total electron density	NHOMO superimposed on total electron density
139		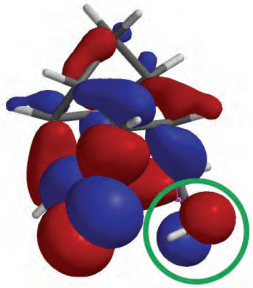	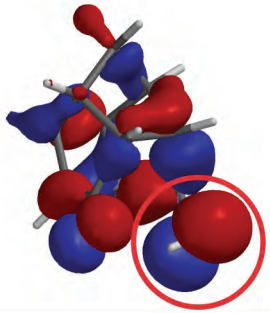	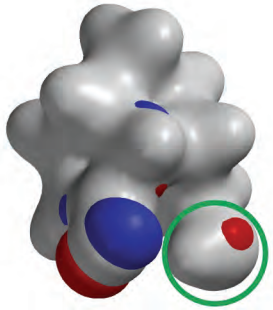	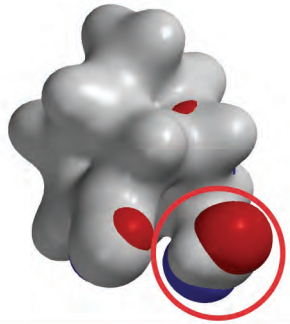
118		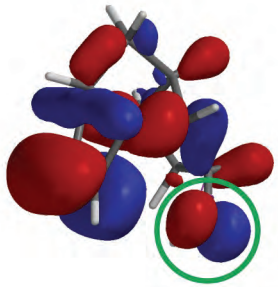	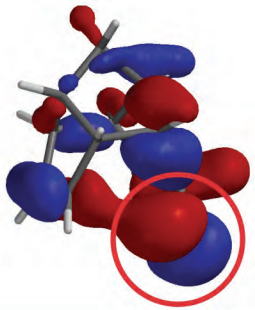	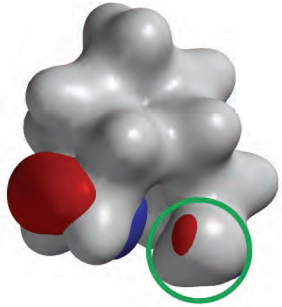	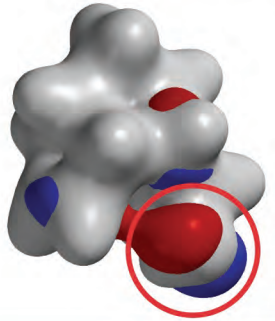
140	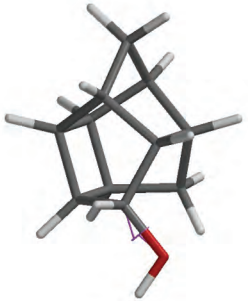	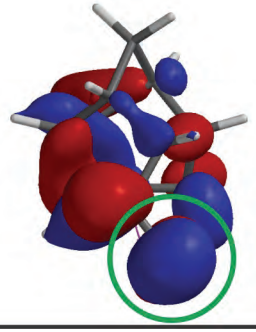	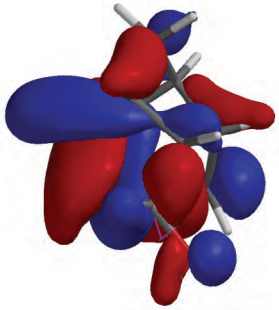	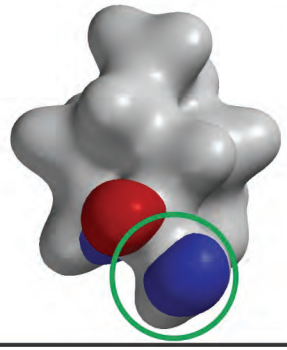	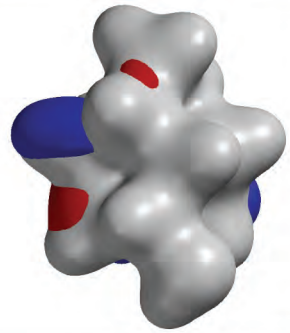

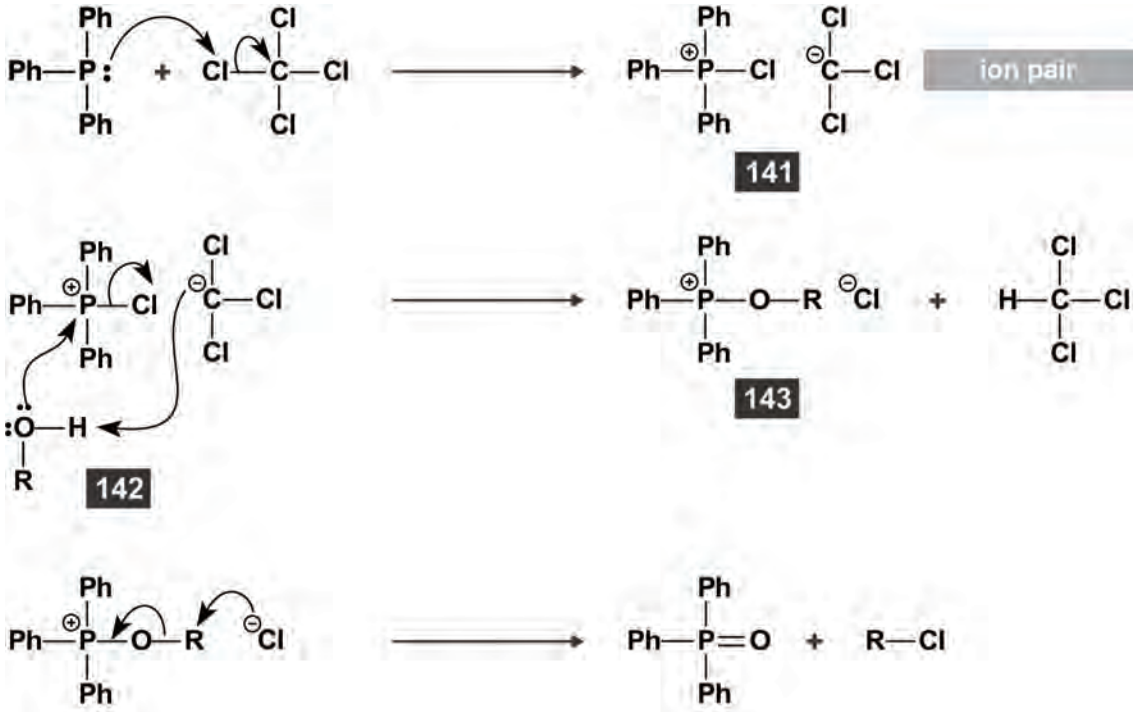

Scheme 2.16[207]**:** Mechanism of the Appel reaction.

It may also be concluded from **Table 2.14** that the HOMO electron densities of the cage hydroxyketones **139** and **134a** are generally concentrated at the carbonyl group. However, these compounds do exhibit significant NHOMO electron density on their hydroxyl group oxygen atoms. There are also literature examples that non-cage hydroxyketones participate in reactions as nucleophilic reagents. Two examples are shown in **Table 2.15**. The HOMO and NHOMO electron densities of these compounds are shown in **Figure 2.11**. Similar to the cage hydroxyketones already examined, these compounds have little HOMO electron densities but much more significant NHOMO electron densities. Suitable NHOMO electron densities seem to be an important factor in nucleophilic additions of hydroxyketones to electrophiles.

Table 2.15: Halogenation of non-cage alcohols

Substrate	Reagents	Conditions	Result	% Yield
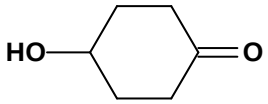 **144**[208]	(i) MsCl, Et_3N (ii) PhSNa	(i) 30 min, 0°C (ii) 4h, 25°C	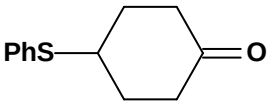	> 75%
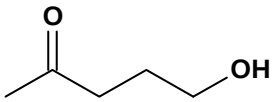 **145**[209]	PPh_3 and CCl_4	30 min, 80°C	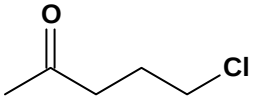	70%

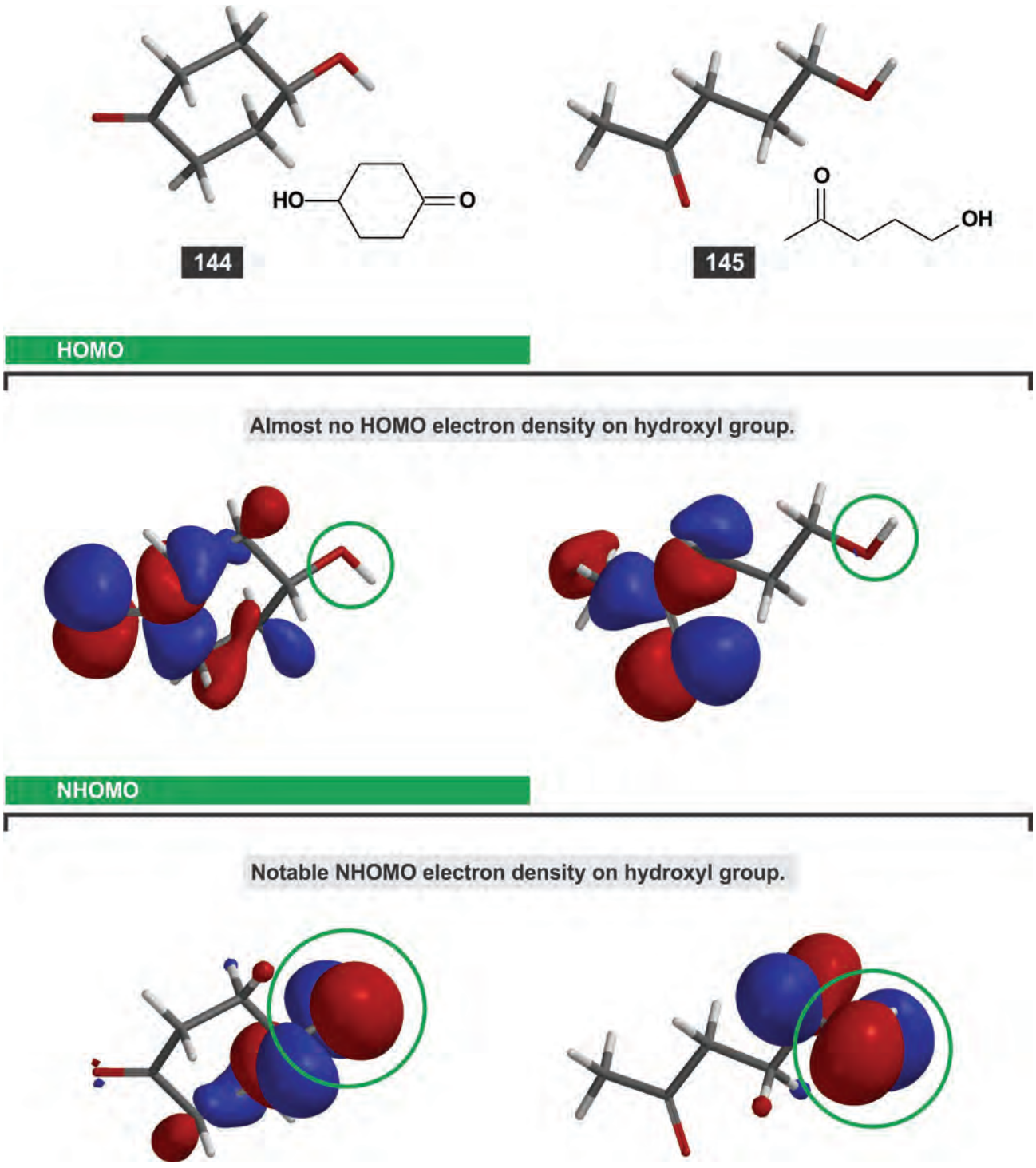

Figure 2.11: The HOMO and NHOMO electron density of **144** and **145**.

The NHOMO electron density on the hydroxyl group of **134a** is significantly smaller than those on **144** and **145**. Also, it should be noted that the HOMO and NHOMO protrusions of **134a** is the smallest of all the substrates considered in **Table 2.14**. Consequently, it is possible that **134a** is not a good nucleophile and thus fails to react with Appel reagents. However, when considering the NHOMO of all these compounds, this conclusion cannot be extended to other cage

hydroxyketones. It is likely that the lack of reaction of cage hydroxyl ketones examined in this study is related to the presence of the PCU framework. The *exo*-orientation of the hydroxyl group in these compounds should make it difficult for the formation of the RO-$PPh_3^+Cl^-$ intermediate **143** due to steric constraints.

Alternative methods to convert **134a/134b** to **135** were sought in the literature (**Table 2.16**). Where possible, the methods were selected based on the fact that they have been applied to alcohols with rigid structures.

Table 2.16: Literature methods used to convert cage alcohols to halogen compounds

Substrate	Reagents	Conditions	Result	Ref.
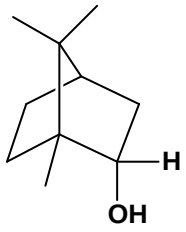 **146**	SeO_2 and TMSCl	Reflux in CCl_4 for 5 hours.	98%	[210]
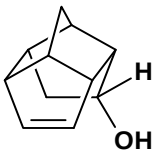 **118**	$POCl_3$	Heated on a steam bath in pyridine for 5 hours.	No yield reported.	[51]
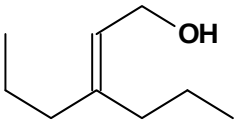 **147**	MsCl and LiCl	In DMF at 0^oC for 1 hour.	80%	[211]

These methods were applied to various cage alcohols. The results of these experiments are summarised in **Table 2.17**.

Table 2.17: Summary of further work convert cage alcohols to halogen compounds

Substrate	Reagents		
	SeO_2-TMSCl	$POCl_3$-py	MsCl-LiCl
134a/134b	No conversion	No conversion	No conversion
139	No conversion	No conversion	No conversion
140	No conversion	No conversion	-

One should note that methods used for halogenation so far in this study function by converting the hydroxyl group into a better leaving group, such as -OMs, $-OPOCl_2$ or -OSeOCl. Unfortunately

these leaving groups are relatively bulky. The conclusions regarding steric problems during the course of the Appel reaction is probably also applicable here.

Subsequently the halogenation potential of thionyl chloride[212-213] was investigated. The reaction of **134a/134b** with $SOCl_2$ in pyridine produced a complex product spectrum with one main product. Analysis of the product spectrum with GC-MS showed that none of these products included halogen atoms in their structures. The reaction of **134a/134b** with neat thionyl chloride produced a mixture of products of which the main product was a halogen compound with *m/z* 134. The product was identified as *endo*-11-chloro-4-isopropylidenepentacyclo-[5.4.0·$0^{2,6}$.$0^{3,10}$.$0^{5,9}$]-undecane-8-one (**148, Scheme 2.17**).

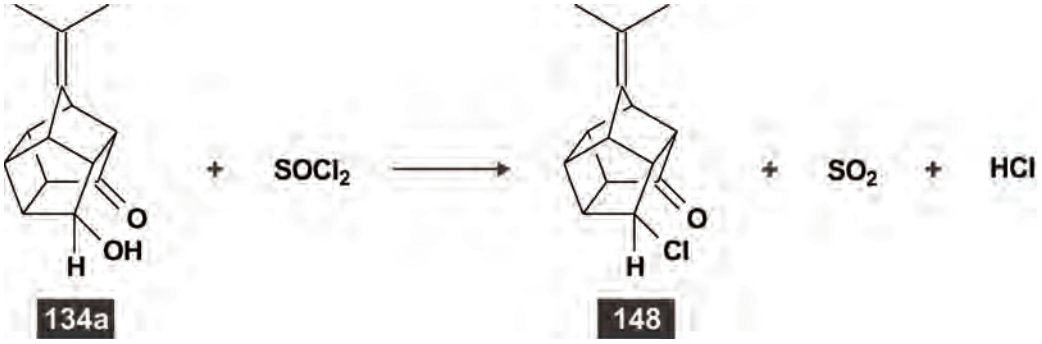

Scheme 2.17: Reaction of **134a** with neat $SOCl_2$.

The assigned structure of **148** is supported by the results of the GC-MS analysis and by the observation that this compound does not react with zinc in acetic acid. It has been shown[51] that zinc in acetic acid affects the reductive dehalogenation of the *exo*-bromoketone **117** (**Scheme 2.18**). The reaction depicted in this scheme will only take place if the halogen atom is in the *exo*-position. Failure of **148** to react with zinc in acetic acid therefore suggests that the chlorine atom of this compound in the *endo*-position. A S_N^i mechanism may be operative in the reaction between **134a** and thionyl chloride.[214]

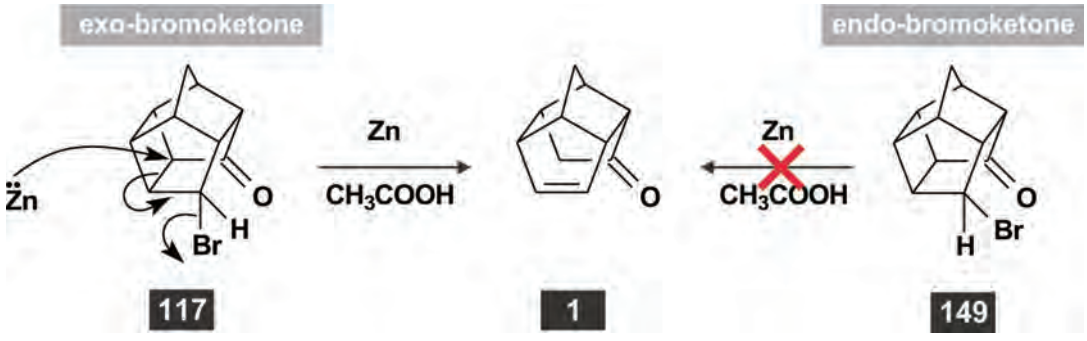

Scheme 2.18[51]**:** Reductive dehalogenation of a cage bromoketone with zinc and acetic acid.

All attempts to substitute the hydroxyl group of **134a** with a halogen atom yielded unsatisfactory results. In a final attempt **134a** was treated with hydrobromic acid. The yield obtained from this reaction was extremely low (2%). As anticipated, substitution of the hydroxyl group coincided with addition of HBr to the double bond. GC-MS analysis of the reaction mixture indicated the presence of approximately equal amounts of two compounds with *m/z* 360. The molecular mass supports a molecular formula of $C_{14}H_{16}Br_2O$ and an absorption at 1736 cm^{-1} in the IR spectrum indicates the presence of a carbonyl group. Four isomers can be formed by the addition of hydrogen bromide to the double bond in **134a/134b** (**Figure 2.12**).

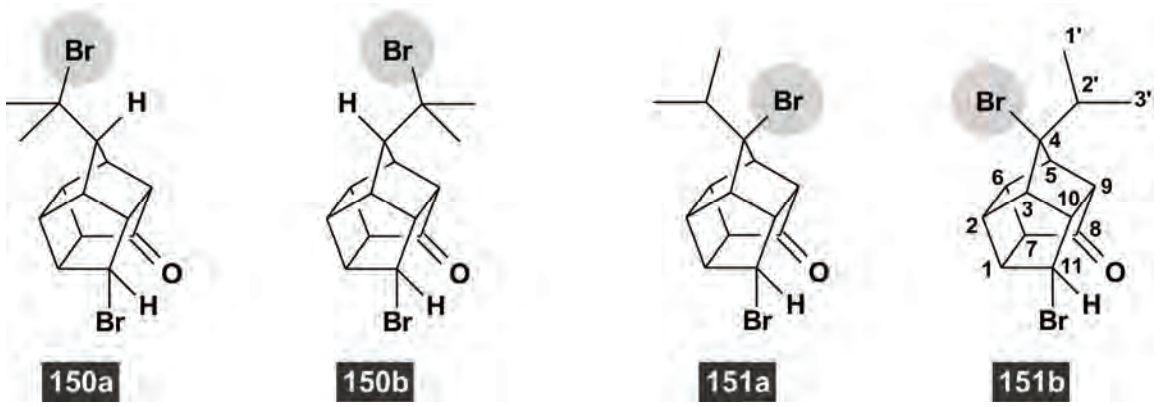

Figure 2.12: Possible products from the reaction of **134a/134b** with hydrobromic acid.

The 150 MHz ^{13}C NMR spectrum ($CDCl_3$) of **150/151** shows signals that may be associated with twenty-eight different carbon atoms. The signals at δ_C 87.0, δ_C 88.4, δ_C 213.36, and δ_C 213.39 represent quaternary carbon atoms. These signals may be assigned to the carbonyl carbon atom (C-8, δ_C 213.36, and δ_C 213.39) and to the bromine-substituted carbon atom (C-4, 87.0, δ_C 88.4). The methine carbon atom bearing the bromine atoms (C-11) registers at δ_C 52.4 and δ_C 53.6 for the two isomers.

It is possible to distinguish between **150** and **151** on the basis of ^1H NMR data. A methine proton at C-4 in structure **150** should register as a singlet. A methine proton at C-2' in structure **151** should register as a heptet. The 600 MHz ^1H NMR spectrum ($CDCl_3$) of the mixture of isomers shows two overlapping heptets at δ_H 1.52 and at δ_H 1.56, which indicates that both products are substituted with bromine at C-4. The methyl groups (C-1' and C-3') of **151** should each register as a doublet. These doublets register at 1.02, 1.07, 1.10, and 2.24 ppm. The signals at δ_H 4.28 and δ_H 4.40 represent the proton attached to the bromine substituted methine carbon atom (C-11). Signals that integrate for sixteen protons register between 2.55 and 2.57 ppm. These signals represent the remaining methine protons. Based on this information, structure **151** was assigned to the mixture of dibromoketones.

The equilibrium mixture of **134a** and **134b** (**Scheme 2.14**, p. 61) consists of approximately 59% of **134a** and 41% of **134b** estimated from ^{1}H NMR data. **Scheme 2.13** shows the HOMO orbitals and Mulliken charges of selected atoms in **134a** and **134b** as determined by molecular modelling (DFT/B3LYP/6-31G**). The alkene functionality of **134b** exhibits the most prominent HOMO lobe and this suggests that protonation may preferably occur at this point during the reaction between **134a/134b** and hydrobromic acid. Consideration of the Mulliken charges indicated on **134b** predicts that protonation at C-2' is more probable than at C-4. It should also be noted that the Mulliken charges indicate that protonation could also occur on the ether oxygen atom in **134b**. However, the HOMO lobe at this point is relatively small and protonation at C-2' is probably still favoured.

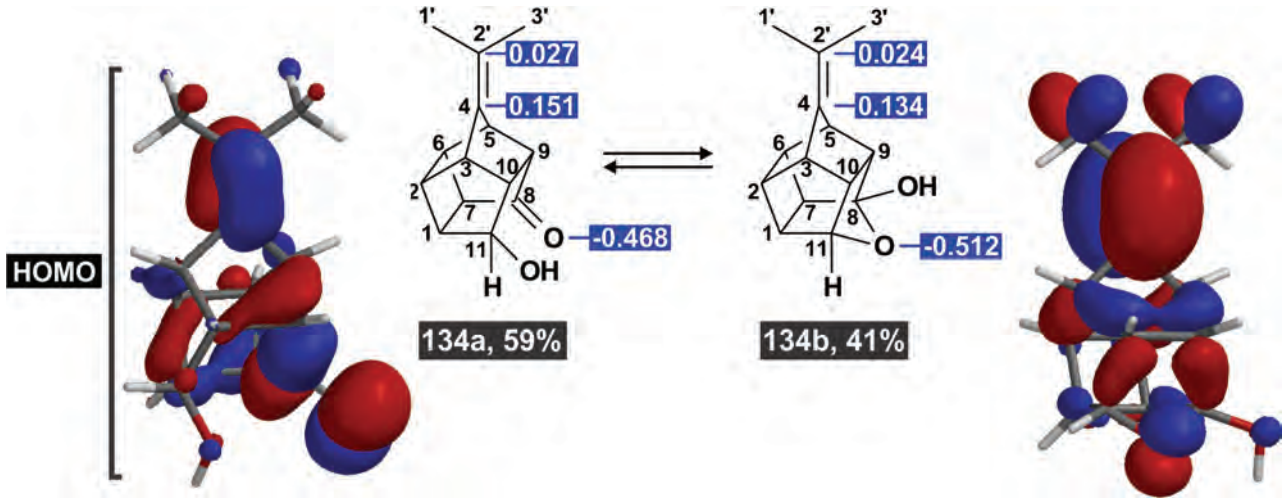

Scheme 2.19: HOMO orbitals and Mulliken charges of selected atoms in **134a** and **134b**

Addition of hydrogen halide to a carbon-carbon double bond proceeds through a carbocation intermediate. Addition of a proton to C-4 or C-2' in **134b** could give rise to the carbocations **152d**, **152e** and/or **152f**. The relative energies of these carbocations are shown in **Figure 2.13**. Comparison of these values beckons the conclusion that carbocation **152f** is the most stable of these three carbocations. Indeed, **152f** appears also to be the most stable carbocation of all the possible carbocations that can be obtained by protonation of the alkene functionalities of **134a/134b**. A possible explanation for the preferred formation of **151a** and **151b** thus appears to be a protonation at C-2' in **134b** followed by the formation of the carbocation **152f** (that precedes **151a** and **151b**). This sequence of events may shift the equilibrium in favour of **134b**. This explanation is in agreement with the results of spectral analysis that show that only **151a** and **151b** are formed during the reaction between **134a/134b** and hydrobromic acid.

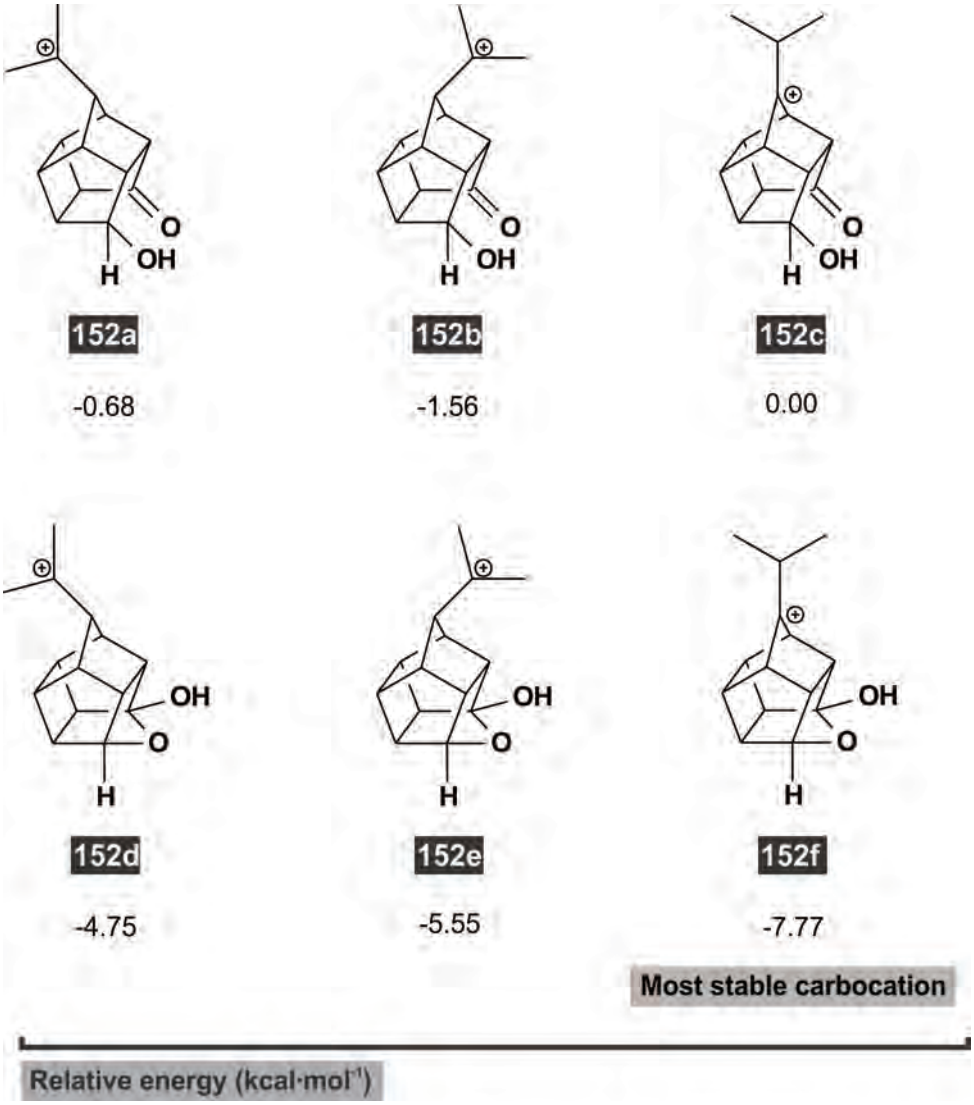

Figure 2.13: Carbocations that could precede the formation of **150** and **151**.

Alternatively, it should be considered that protonation of the carbonyl oxygen atom and/or the alkene functionality in **134a** is also probable. However, protonation of the oxygen atom of the carbonyl group seems more probable due to the larger size of this HOMO lobe compared to that on the alkene functionality. Also, the lobe on the oxygen atom appears to be more accessible than that on the alkene functionality. It has been reported[147] that the transformations of PCU γ-hydroxyketones to their corresponding PCU hemiketals are catalysed by acid. A possible mechanism for this transformation is presented in **Scheme 2.20**. In conclusion, it seems that pathways exist for both **134a** and **134b** to be transformed to the carbocation **152f** that precedes the observed products **151a** and **151b**.

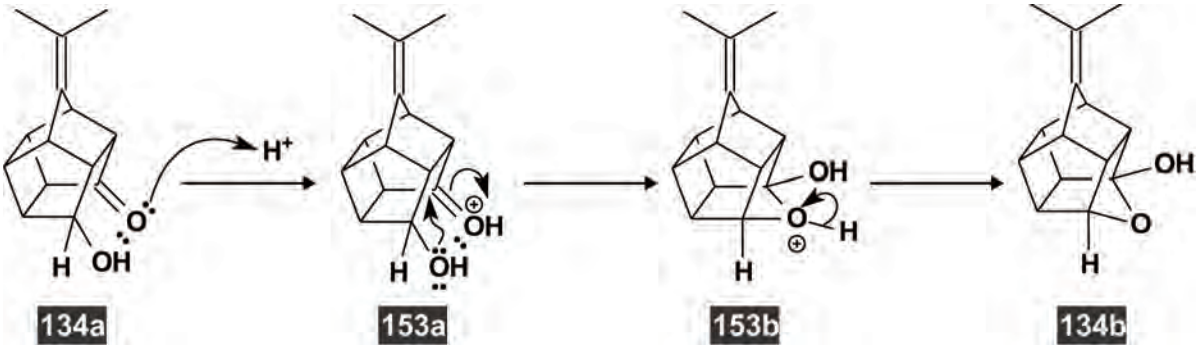

Scheme 2.20: Possible conversion of **134a** to **134b**.

Treatment of the dibromoketone **151** with zinc in refluxing acetic acid was expected to produce the cage alkene 10-isopropyltetracyclo[6.3.0·0^{4,11}.0^{5,9}]undec-2-en-6-one (**155, Scheme 2.21**). Instead, a material was produced that could not be satisfactorily analysed. The material was dissolved in DMSO but precipitated inside the NMR tube during the analysis. Due to poor solubility in conventional NMR solvents no NMR data were obtained. Absorptions at 2990 cm^{-1} and 1740 cm^{-1} in the IR spectrum indicated the presence of a carbonyl group and olefinic hydrogen atoms in the material.

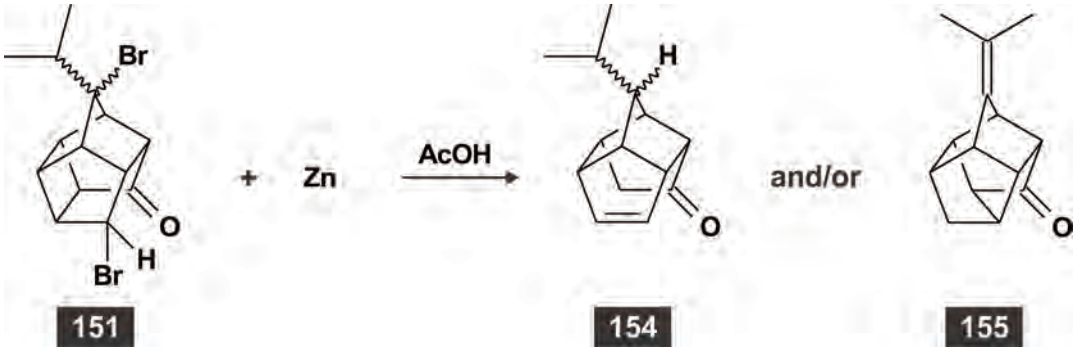

Scheme 2.21: Possible outcomes of reductive dehalogenation of **151**.

It was found that some of the components of the mixture dissolved in pyridine. Analysis of the pyridine solution with GC-MS showed the presence of a mixture of compounds. It was found that the composition of the mixture was extremely sensitive to the reaction conditions employed. Variation of the reaction time and temperature changed the ratio of products either towards those with *m/z* 200 or towards those with *m/z* 202. **Figure 2.14** shows a typical result obtained from GC-MS analysis and possible structures with molar masses in agreement with the molar masses obtained from this analysis. During a systematic study no reaction conditions could be found that significantly simplified the product spectrum. It may be concluded that the system is more prone to by-product formation under acid conditions than the PCU system. Two milder reagent systems,

zinc in methanol and zinc in saturated ammonium chloride solution,[215] were used in an attempt to lessen the extent of by-product formation. Neither of these reagents reacted with **151**.

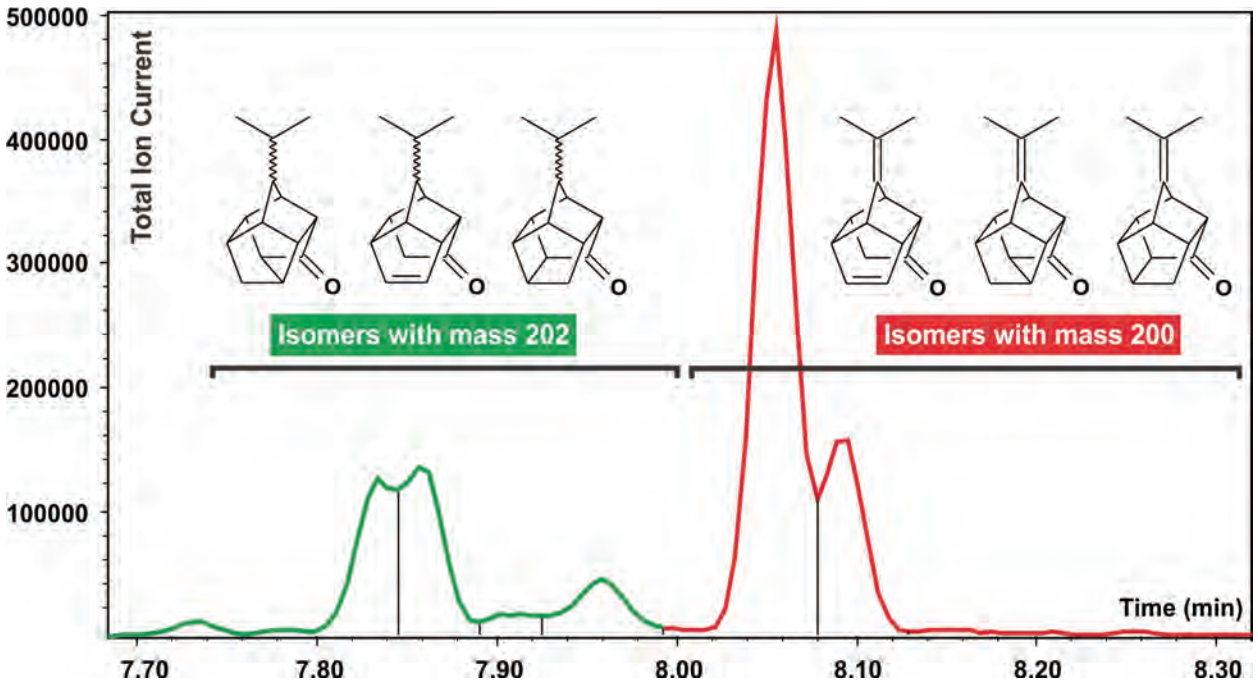

Figure 2.14: Possible products from the reaction of **151** with zinc and acetic acid.

Methods to convert **134a/134b** to an iodine compound were briefly investigated during this study. The results of these reactions are summarised in **Table 2.18**.

Table 2.18: Methods used for conversion of 135a/135b to an iodine compound

Substrate	Reagents	Conditions	Result	Ref.
134a/134b	$CeCl_3 \cdot 7H_2O$/NaI over SiO_2	Microwave irradiation, no solvent	No conversion	[216]
134a/134b	PPh_3/I_2	Microwave irradiation, no solvent	No conversion	[217]
134a/134b	CH_3SO_3H/NaI	In acetonitrile at room temperature.	No conversion	[218]

In conclusion, the attempts to synthesise new cage alkenes from **1** and **23** yielded only one suitable candidate, i.e. **127**. This compound was subsequently further investigated for ROMP reactivity. The low success rate experienced during this part of the study necessitated the identification of alternative cage alkenes from the literature to facilitate the ROMP study presented in **Chapter 3**.